Single particle trajectories inside the PFRC with Odd Parity Rotating Magnetic Field

Hyaline Chen

1 Introduction

The Princeton Field Reversed Configuration is a high-β, compact fusion reactor design, which utilizes an odd Rotating Magnetic Rield (RMF_o), to form and heat up the plasma. Inside the central cell of the PFRC, the plasma interacts with the RMF. It has been shown previously that the addition of a odd rotating magnetic field preserves the closure of the field lines in a FRC [2].

However, the single particle trajectory picture do not have to agree exactly with the field line picture, with many particle trajectories not following the field lines exactly. High energy particles are an example, since the gyroradius is so large that the particles' trajectories do not have to follow field lines at all. By High energy particles in this paper, we mean particles with $E > 1000eV$, one reason for this definition is that we find when heating a low energy particle started with $E \sim 2eV$ there is a saturation in its heating, with maximum energy capped at around 1000 eV. Therefore it is of our interest of both what happens to particles started below and above this energy boundary.

The magentic field of the FRC has two magnetic nulls, one at the top and botton called the x-points, and one in the midplane called the o-point. The Hill's vortex solution equations for FRC magnetic field are (from Glasser equations):

$$A_\phi = \frac{\psi_0}{r}\left(\frac{r^2}{r_s^2}\right)\left(1-\frac{r^2}{r_s^2}-\frac{z^2}{z_s^2}\right), A_z = 0, A_r = 0 \tag{1}$$

$$\psi_0 = B_0 r_s^2/2 \tag{2}$$

$$B_r = -B_0\frac{rz}{z_s^2} \tag{3}$$

$$B_z = -B_0\left(1-\frac{2r^2}{r_s^2}-\frac{z^2}{z_s^2}\right) \tag{4}$$

$$\tag{5}$$

So the null points are:

$$\text{For} \quad B_r = 0 \quad \text{either} \quad z = 0 \quad \text{or} \quad r = 0 \tag{6}$$

$$\text{if} \quad z = 0 \quad \text{(the o-point)}, \quad B_z = -B_0\left(1-\frac{2r^2}{r_s^2}\right) = 0 \rightarrow 2r^2 = r_s^2 \rightarrow r_o = \frac{r_s}{\sqrt{2}} \tag{7}$$

$$\text{if} \quad r = 0 \quad \text{(the x-point)}, \quad B_z = -B_0\left(1-\frac{z^2}{z_s^2}\right) = 0 \rightarrow z_x = \pm z_s \tag{8}$$

The equations for the odd RMF are:

$$\psi \equiv \phi - \phi_0 - \omega t, \quad \xi \equiv kr \tag{9}$$

$$A_r = \frac{2B_0}{k} I_0(\xi)\cos kz \sin\psi \tag{10}$$

$$A_\phi = \frac{2B_0}{k} I_0(\xi)\cos kz \cos\psi \tag{11}$$

$$A_z = -\frac{2B_0}{k} I_1(\xi)\sin kz \sin\psi \tag{12}$$

From the vector potentials we can derive the induced electric field and magnetic field.

$$E = -\frac{\partial A}{\partial t} \tag{13}$$

$$B = \nabla \times A \tag{14}$$

$$B_r = 2B_0 \left[I_0(\xi) - \frac{I_1(\xi)}{\xi} \right] \sin kz \cos \psi \tag{15}$$

$$B_\phi = 2B_0 \frac{I_1(\xi)}{\xi} \sin kz \sin \psi \tag{16}$$

$$B_z = 2B_0 I_1(\xi) \cos kz \cos \psi \tag{17}$$

Plotting these equations in Mathematica, the results of the FRC, RMF, total B field, and the induced electric field can be found in Figure 1, 2, and 3. In figure 1 we see separately the field lines for the RMF and FRC fields. One can see the null points are where the magnetic field lines changed directions. The RMF field rotates in the x-y plane and deforms in shape in the x-z plane. Magnetic field does no work, hence the heating of the particles primarily depends on the electric field induced by the RMF. In the midplane, as shown in Figure 3, the electric field always points in the same direction and rotates with time. Outside the midplane, the shape of the electric field is shown in Figure 2.

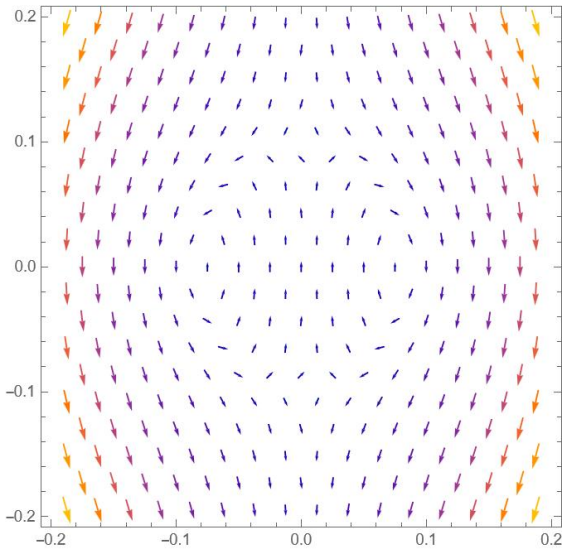

(a) the shape of the FRC B field without RMF, the length of the arrows represents the magnitude

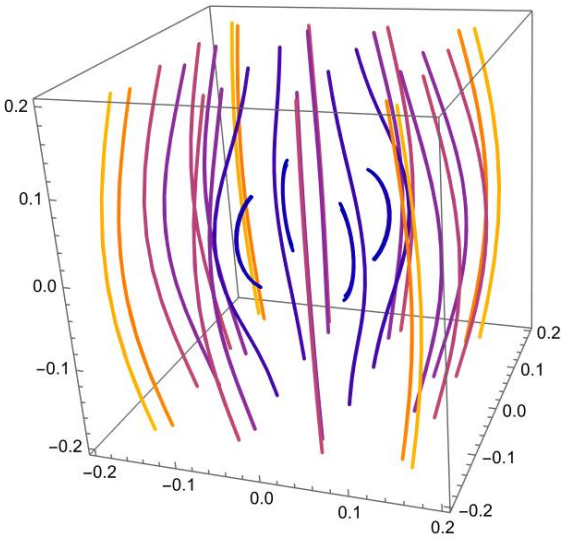

(b) 3D plot of the total B field, color represents magnitude

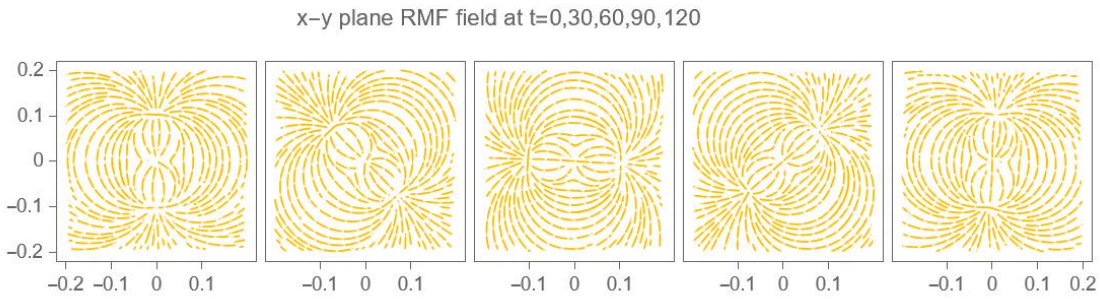

(c) z=0 plane plot of RMF B field at three different times

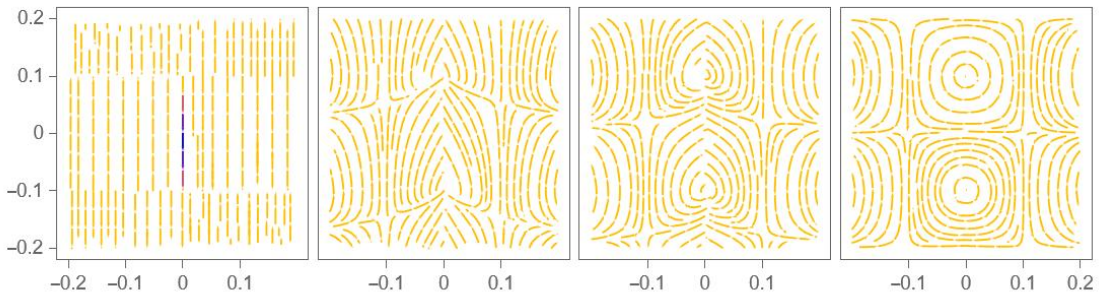

(d) y=0 plane plot of RMF B field at three different times

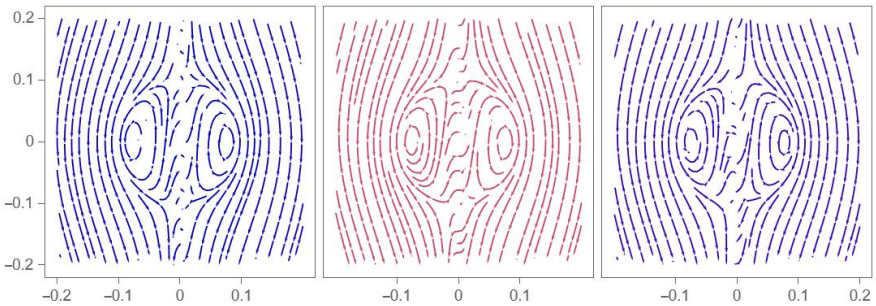

(e) y=0 plane plot of total B field at three different times

Figure 1

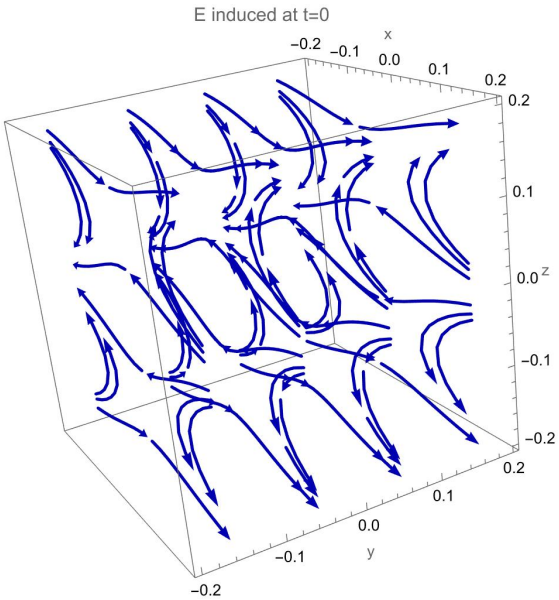

(a) 3D plot of the shape and direction of the RMF induced electric field

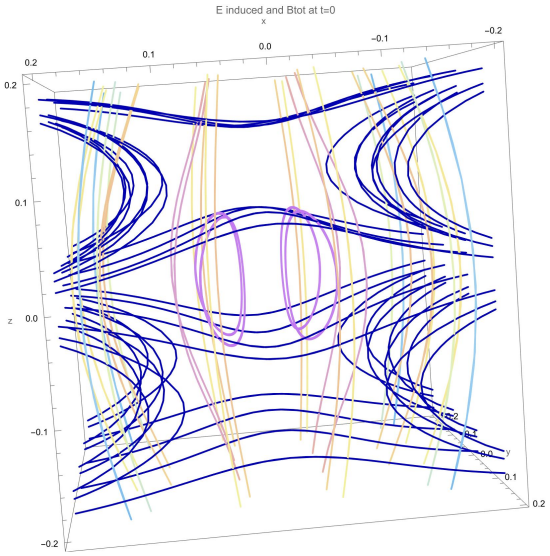

(b) 3D plot of the shape and direction of the RMF induced electric field with the original FRC field lines, blue lines are the induced electric field and other colors represent the FRC field with different strength of B

Figure 2

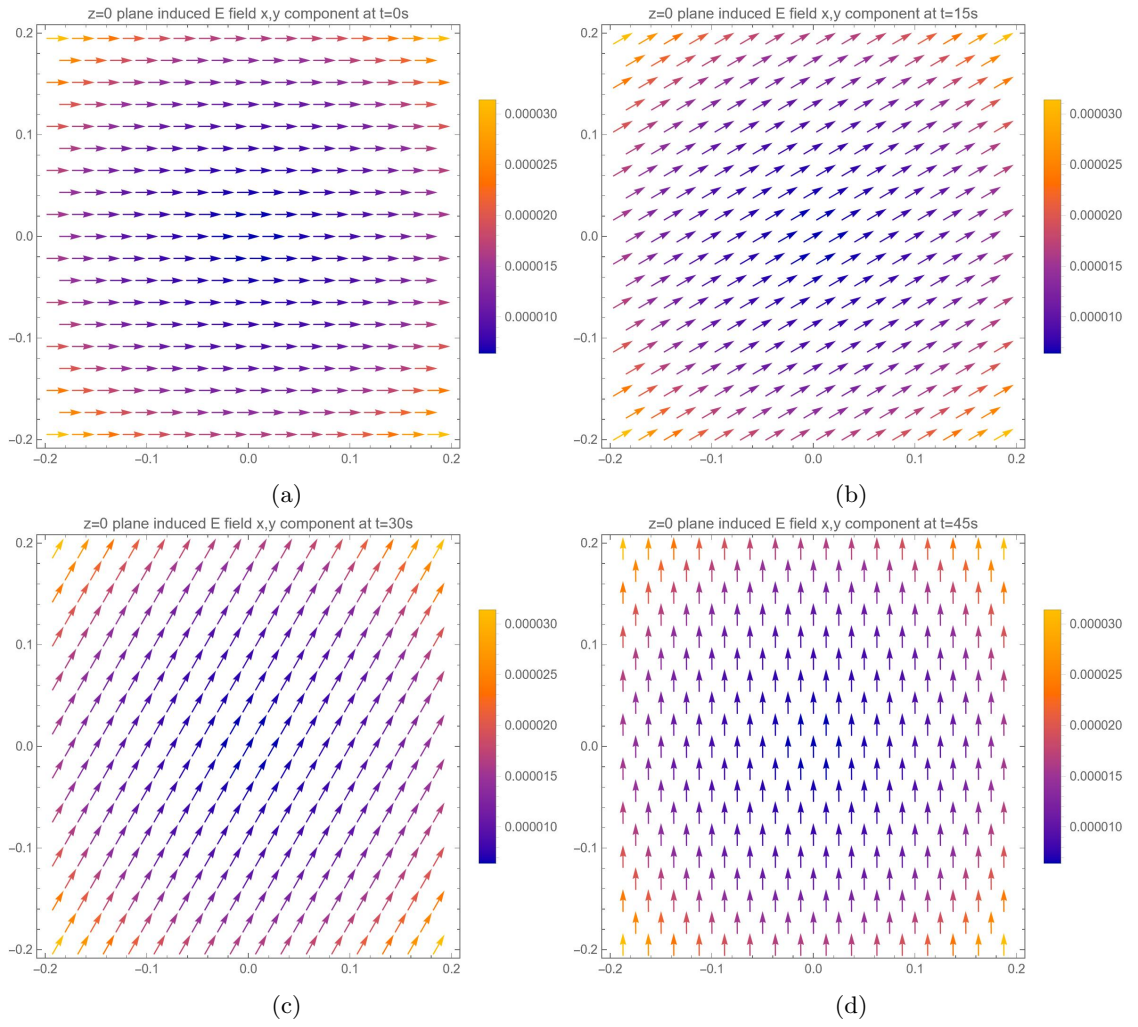

Figure 3: The electric field in the z=0 midplane at different times

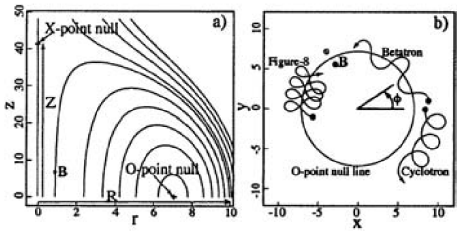

Figure 4: (a) Shape of FRC magnetic field in z-r plane, Kappa = 4:1. (b) Shapes of typical cyclotron, betatron, and figure-8 orbits in z = 0 plane. [4]

There have previously been studies of low energy ion trajectories inside the PFRC with RMF [3]. The midplane with z=0 is a stable subspace even with the addition of an odd RMF, meaning that particles started with no z direction velocity and position will stay confined in the midplane. The main classes of orbits in the z=0 subspace are cyclotron orbits inside and outside the o-point, the betatron orbits and figure-8 orbits around the o-point; betatron orbit's phi velocity does not change sign where a figure-8 orbit does. Figure 8 orbit is studied in a low bo (bo/b0 $< 10^{-3}$) setting and the energy gain is approximately calculated [4]. Cohen and Landsman showed that figure 8 orbits gains significant energy from interaction with the RMF from stochastic heating, since it is more nonlinear and can gain energy even at small bo/b0 ratio [1].

In this report, Section 2 describes the possibility of losing particles with follows closed field lines. Section 3 discusses a possible mechanism through which a low energy, heated particle may gain z momentum, leading to its loss. Section 4 presents the batch run results from the single particle RMF code written by Alan Glasser, divided into behaviours of higher energy ($\geqslant 1000eV$) particles and those with lower energies.

2 Lost of cyclotron particles

Even if field lines are closed, and a particle seems to initially follow the field lines inside the FRC without RMF, in cyclotron orbit gyrating around the field lines, does this mean that the particle with stay confined?

Running simulations with the following initial conditions, we see that if the initial rfac is too small or too close to the separatrix, even if the cyclotron orbit follows the original, closed field line, it could get lost. This is because of the particles' gyroradius being smaller than the length difference between the particle's followed closed field line and its closest open field line. Hence, the particle may stray to follow the neighbouring open field lines and gets lost.

parameters	values
b_0 (FRC)/G	1000
r_s (FRC)/cm	5
κ (FRC)	2
ϕ_0	90
θ_0	80
z_{fac}	0
r_{fac}	0.1, 1.47, 1.46, 1.48
E_0 /eV	2
escape factor	2

Table 1

In figure 5 (a) and (b) we see a particle that follows a field line close to the separatrix, one starting from the left side and one from the right. We see that although the particle initially follows the field line closely, at the top or bottom where the behaviour of neighbouring field lines diverge from its own field line, the particle reaches open field lines and gets lost. In contrast, in Figure 5 (c) and (d) we have one particle which follows a closed field line completely, which is far enough from open field lines to stay on its original orbit, and another particle following an open field line originally and gets lost because of that. This suggests the importance of the gyroradius.

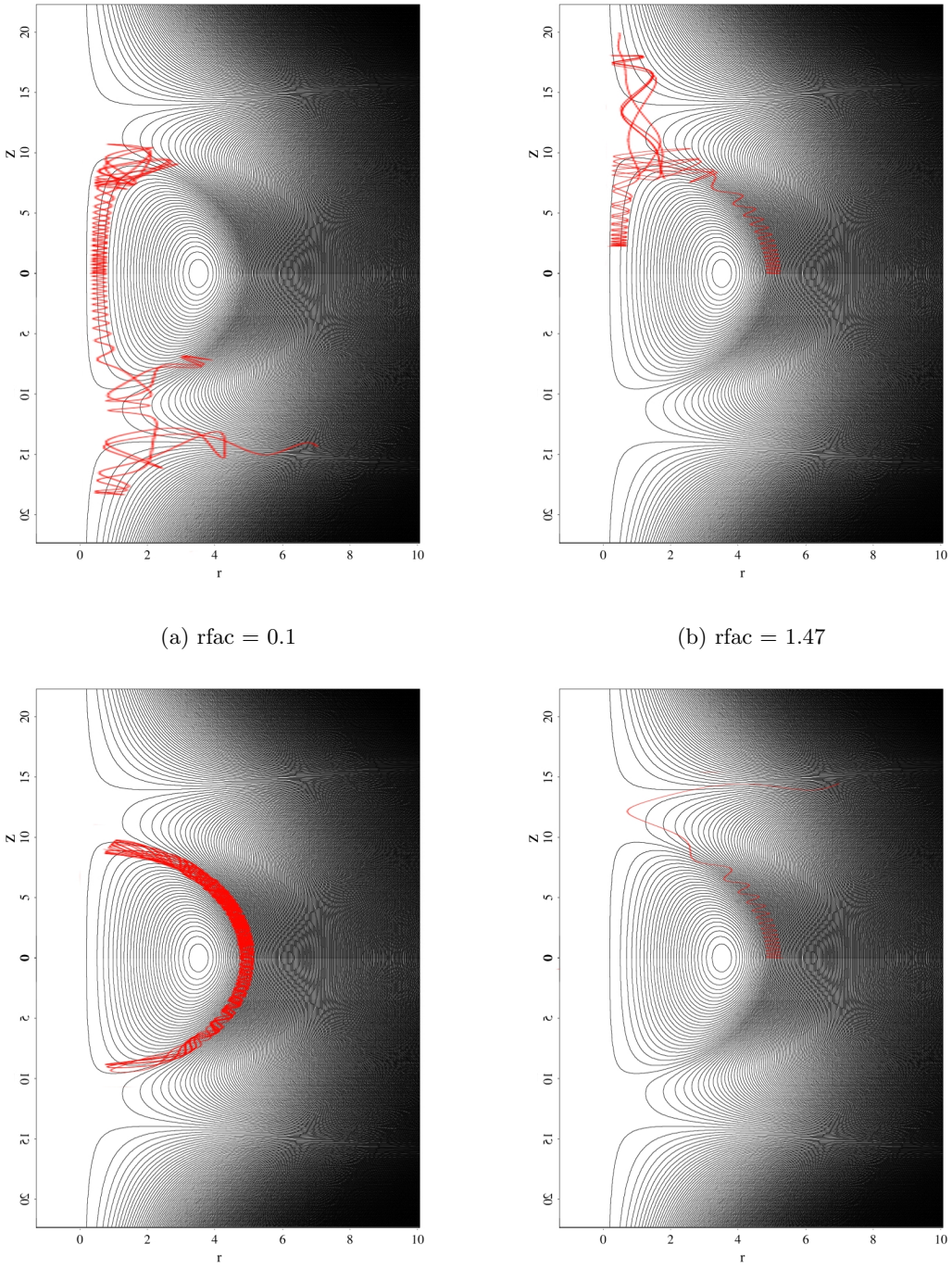

(a) rfac = 0.1

(b) rfac = 1.47

(c) rfac = 1.46

(d) rfac = 1.48

Figure 5: The single particle simulation in FRC without RMF for different starting rfac

3 The increase in the z-direction oscillation of heated low energy ions

For a particle with RMF which stays confined (betatron orbits and some cyclotron and figure 8 orbits, for example), we sometimes see changing amplitude in its z direction oscillation. This mechanism contributes to the loss of particles as the particles with large z displacements can get

lost in the field line openings near the top and bottom cusps.

Is this a behaviour unique to the particles inside a RMF field? Do particles inside a FRC without RMF exhibit similar behaviours? Using the Hamiltonian of a particle in magnetic field, we can solve for its equation of motion inside an FRC.

$$H = \frac{1}{2m}\left[(p_r)^2 + (p_z)^2 + \left(\frac{p_\phi}{r} - \frac{q}{c}A_\phi\right)^2\right] \tag{18}$$

$$= \frac{1}{2m}\left[(p_r)^2 + (p_z)^2 + \left(\frac{p_\phi}{r} - \frac{qB_0 r}{2c}\left(1 - \frac{r^2}{r_s^2} - \frac{z^2}{z_s^2}\right)\right)^2\right] \tag{19}$$

Defining the dimensionless constants

$$\rho \equiv \frac{r}{R} \tag{20}$$

$$b \equiv \frac{qB_0}{2c} \tag{21}$$

$$p_\rho \equiv \frac{p_r}{bR} \tag{22}$$

$$P \equiv \frac{p_\phi}{bR^2} = constant \tag{23}$$

$$F \equiv \frac{b^2R^2}{2m} \tag{24}$$

We can rewrite the equations and use Hamilton's equations to derive the equations of motion in z and r. Note that p_ϕ is conserved because of the symmetry in the ϕ direction.

$$H = F[p_\rho^2 + p_\zeta^2 + (\frac{P}{\rho} - \rho(1 - \rho^2 - \zeta^2))^2] \tag{25}$$

$$\dot{r} = \frac{\partial H}{\partial p_r} = \frac{\partial H}{\partial p_\rho}\frac{1}{bR} = \frac{p_r}{m} \tag{26}$$

$$\rightarrow m\dot{r} = p_r \tag{27}$$

$$m\dot{z} = p_z \tag{28}$$

$$\dot{p_r} = m\ddot{r} = -\frac{\partial H}{\partial r} = -\frac{\partial H}{\partial \rho}\frac{1}{R} = -\frac{2F}{R}(\frac{P}{\rho} - \rho(1 - \rho^2 - \zeta^2))(-\frac{P}{\rho^2} - (1 - \rho^2 - \zeta^2) + 2\rho^2) \tag{29}$$

$$\dot{p_z} = m\ddot{z} = -\frac{\partial H}{\partial z} = -\frac{\partial H}{\partial \zeta}\frac{1}{Z} = -\frac{2F}{Z}(\frac{P}{\rho} - \rho(1 - \rho^2 - \zeta^2))(2\rho\zeta) \tag{30}$$

$$\tag{31}$$

So we have the equations of motion, two coupled second order differential equations.

$$\ddot{\rho} = (\frac{2F}{mR^2})(\frac{P}{\rho} - \rho(1 - \rho^2 - \zeta^2))(\frac{P}{\rho^2} + 1 - 3\rho^2 - \zeta^2) \tag{32}$$

$$\ddot{\zeta} = -(\frac{4F}{mZ^2})\zeta(P - \rho^2(1 - \rho^2 - \zeta^2)) \tag{33}$$

Using a simple generic orbit $\rho \sim \frac{R}{2} + R\cos\omega_{ci}t$, which represents betatron and figure-8 orbits, and solving equation (28) numerically, we obtain an regular periodic oscillation in the z direction with constant amplitude. Part of the numerical solution graph is presented in Figure 5.

We hence see that the FRC only gives rise to regular amplitude oscillations in the z direction for figure-8 and betatron orbits, as consistent with results of simulations. So this behaviour is unique to the FRC with RMF.

Which component of the RMF might have contributed to this effect? The first guess maybe that the z direction electric field increases the z momentum. However, running simulations with the z direction electric artificially turned off, similar behaviours are still observed. So although E_z could have contributed to it, there are other mechanisms. Then, we consider the Lorentz force due

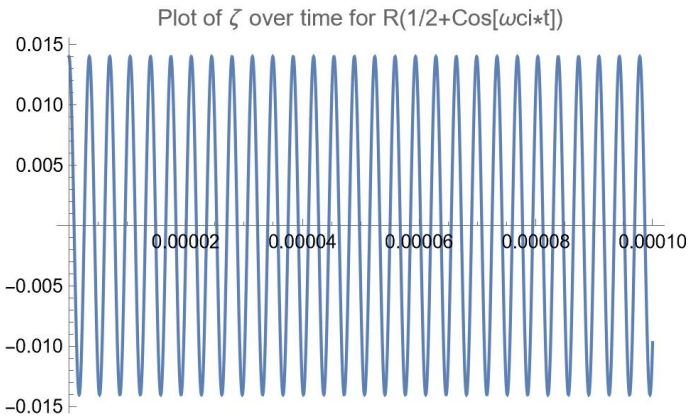

Figure 6

to the RMF magnetic field. either $v_\phi \times B_r$ or $v_r \times B_\phi$ could give a force in the z direction which alters the z velocity thus amplitude.

$$B_r = 2B_0[I_0(\xi) - \frac{I_1(\xi)}{\xi}]\sin kz\cos\psi \tag{34}$$

$$B_\phi = 2B_0\frac{I_1(\xi)}{\xi}\sin kz\sin\psi \tag{35}$$

$$\tag{36}$$

Take a look at the r magnetic field. we have

$$F_z = qv_\phi \times B_r = qv_\phi \times 2B_0[I_0(\xi) - \frac{I_1(\xi)}{\xi}]\sin kz\cos\psi$$

Suppose the r and $\cos\psi$ average to a constant in the time scale of the z direction oscillation (z oscillation period longer than r and phi direction oscillation periods). Then we have $B_r \propto \sin kz$ and so

$$F_z = m\ddot{z} = -ev_\phi B_{r0}\sin kz$$

Suppose v_{phi} is also constant, then we have the equation for a pendulum, giving regular oscillation with constant amplitude. However, in most simulations it can be seen that $p_\phi \propto v_{phi} \propto Energy$. Hence, oscillations in energy, resulting in oscillations in the phi velocity, could be a mechanism with which z-direction oscillation becomes irregular.

For example, when a particle is doing oscillation around the midplane up and down, and when it returns to the midplane from above, there is suddenly a surge in its energy, then $\ddot{z}$ surges with v_ϕ, giving the particle an extra z momentum since the restoring force is stronger than before. Then, if the energy surge flattens before the particle reaches the midplane, the particle's gained extra momentum would not be lost. There is then a net increase in its z momentum.

We can estimate the impulse gained from such a energy spike.

$$\Delta I = \Delta(\int F dt) \tag{37}$$

$$= \int_0^{\frac{1}{4}T_z} ev_\phi B_{r0}\sin kz(t)dt + \int_{\frac{1}{4}T_z}^{\frac{1}{2}T_z} ev_{\phi 0}B_{r0}\sin kz(t)dt \tag{38}$$

For the parameter values used in the PFRC in SI units, kz << 1, so we can expand the sin(kz). We can also approximate z by a generic oscillation term.

$$\sin kz \sim kz, z \sim A_z \cos \omega_z t \tag{39}$$

$$\Rightarrow \Delta I = \int_0^{\frac{1}{4}T_z} ev_\phi B_{r0} k A_z \cos \omega_z t dt + \int_{\frac{1}{4}T_z}^{\frac{1}{2}T_z} ev_{\phi 0} B_{r0} k A_z \cos \omega_z t dt \tag{40}$$

$$= \frac{1}{\omega_z} ev_\phi B_{r0} k A_z - \frac{1}{\omega_z} ev_{\phi 0} B_{r0} k A_z \cos \omega_z t \tag{41}$$

$$= \frac{1}{\omega_z} eB_{r0} k A_z (v_\phi - v_{\phi 0}) = m\Delta v_z \tag{42}$$

$$\Delta v_z = \frac{eB_{r0}}{m} \frac{kA_z}{\omega_z} \Delta v_\phi \tag{43}$$

$$\tag{44}$$

Define

$$\frac{eB_{r0}}{m} \equiv \omega_{ci,r0}$$

Then we have

$$\Delta v_z \sim (2\pi \frac{\omega_{ci,r0}}{\omega_z} \frac{A_z}{\lambda_{RMF}}) \Delta v_\phi$$

A similar result can be derived on the correspondence between the change in z velocity and the change in r velocity in this case. This mechanism can also lead to a loss of z momentum if the energy surge occured when the particle is travelling away from the midplane. Therefore, if the period of energy fluctuation interacts regularly with the period of oscillation of the particle in the z direction, there is no net gain in z momentum. However, if there is misalignment, net momentum can be obtained.

In Figure 7 we see a particle lost because of its suddenly increasing z momentum. We see that p_ϕ is almost identical in trend as the energy, and during the final surge of p_z through which the particle is lost, there is a corresponding spike in its energy.

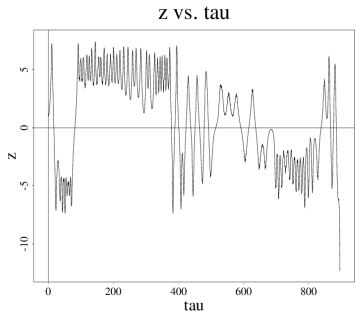

(a)

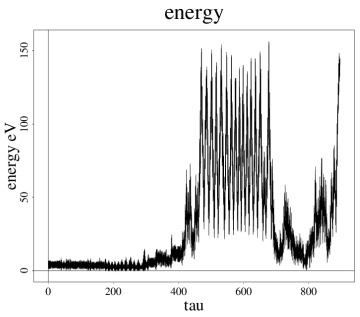

(b)

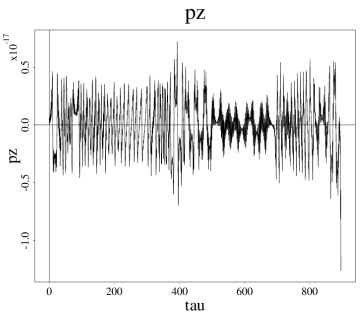

(c)

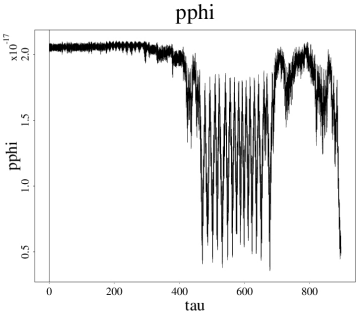

(d)

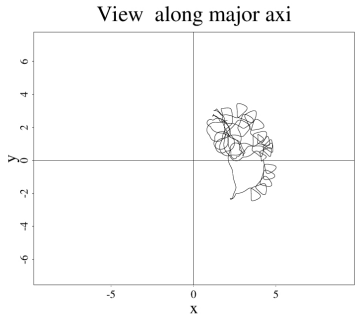

(e)

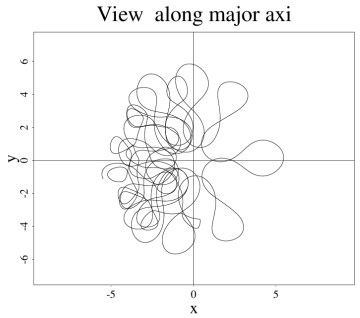

(f)

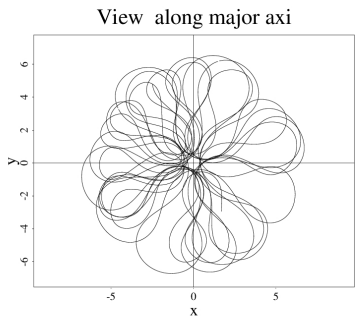

(g)

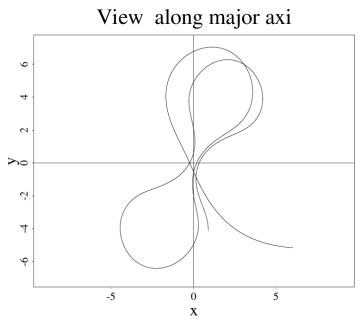

(h)

Figure 7

4 batch run results

This section summarizes my findings running batch/single particle runs with the RMF code written by Alan Glasser. The RMF code is a single-particle trajectory simulation assuming the solution of a Hill's Vortex inside the separatrix, and for the purpose of this report the external field obeys the Zakkharov boundary conditions.

The report is divided into two subsections, firstly discussing high energy ions with energies from 1000 eV upwards, later discussing lower energy ions with energy of around 2eV. Low energy ions are the more usual occurrence, which we wish to heat up using the Rotating Magnetic Field (RMF). While the higher energy particles may be produced by mechanisms beyond the single particle simulation like by collision with other more energetic particles in the higher tail end of the velocity distribution of ions.

We explore the effects of different initial variables on the heating and confinement of ions, in a FRC configuration with kappa = 2 and rs = 5cm or 7cm; the omfac of the RMF is set to either 1.1 or 1.5, and the escape factor is set to 2. Initial phase of the RMF is set at 90 degrees.

For all graphs below, the color gradient from green to red demonstrates increasing values of the other variable. For example, if energy0 and rfac are the two independent variables on the x-axes of a set of graphs, the colors on the graphs where energy0 is the x-axis represents increasing rfac according to the step size given, vice versa.

4.1 High energy ions

4.1.1 z=0 subspace high energy ions (Energy0 = 1300-3300 eV)

parameters	values
omfac	1.1
b_0 (FRC)/G	1000
b_o (RMF)/G	10
r_s (FRC)/cm	7
κ (FRC)	2
ϕ_0	90
θ_0	90
z_{fac}	0
r_{fac}	0.1 - 1.7 (step size 0.1, 16 steps)
E_0 /eV	1300 - 3300 (100, 20)
τ_{max}	5000
escape factor	2

Table 2

From Figure 1 (a) and (c), it can be seen that for E0 > 2300 eV there is little dependence of average energy on rfac, for even lower energies, however, there are fluctuations in average energy. For E0 = 1300 for rfac < 0.3 there is a decrease in the average energy for about 1000 eV. In terms of the maximum energy, on average, the higher the rfac the higher the maximum energy of the particles, with some fluctuations at smaller rfac.

Shown in Figure 1 (f), for high energy ions (E0=1300-3300), the average energy increases with initial energy overall in the z=0 subspace. The maximum energy also shows such a positive correlation. The black line in the average energy versus E0 plot (f) is the identity line equaling the initial energy. The graph shows that for $E0 < 2000$ the average energy is below the original energy for almost all starting rfac values. However, for $E0 > 2500$ some particles starts to gain energy on average. On average for particles with small rfac, a significant energy lost can be observed. For example, starting with rfac=0.6, single particle simulations in the midplane show particles with

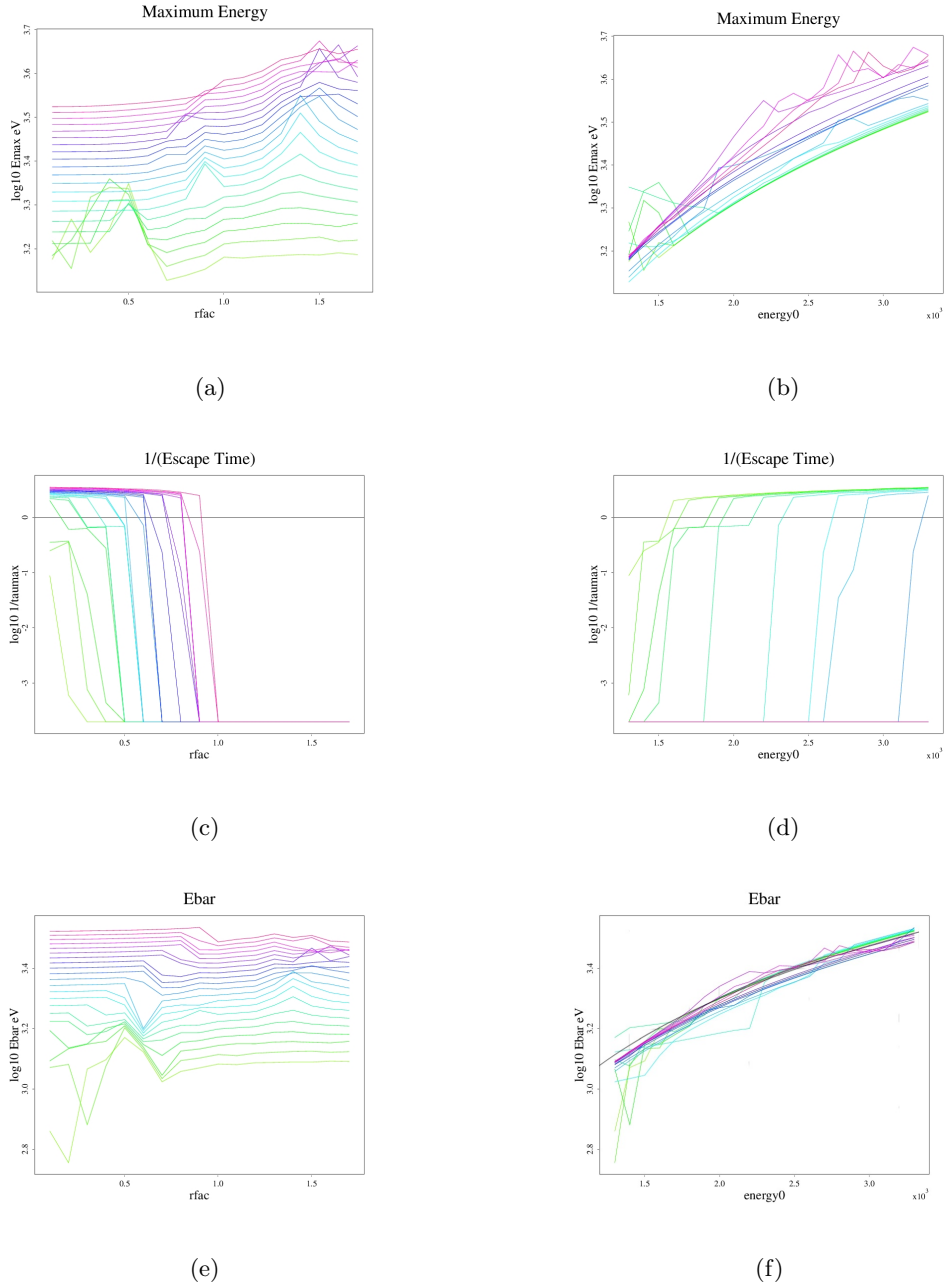

Figure 8: the black line in (f) is added, it shows the original energy

starting energy of 2000 eV but average energy of only $\sim$ 1500 eV, as can be seen in figure 2a. The corresponding betatron orbit is shown on the right.

As for the escape time, as shown in figure 1c, at each energy level above saturation, there is a sharp increase in the confinement time at a critical rfac, as rfac gets bigger. The high energy ion orbits suddenly become very stable at a cutoff rfac in the z=0 subspace. As energy increases the cutoff rfac increases.

This stable class of orbit is desirable because it has almost the same average energy and higher maximum energy as the escaped orbits.

To see where the sharp increase in confinement comes from, single-particle simulations where particles escape and not escape are run, and the results are compared. Figure three shows an example of escaped particle orbit. One sees that the particle is lost on the side because of the

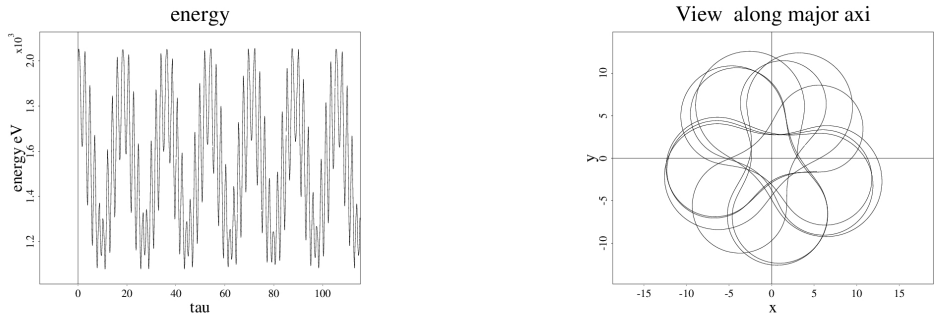

(a) (b)

Figure 9

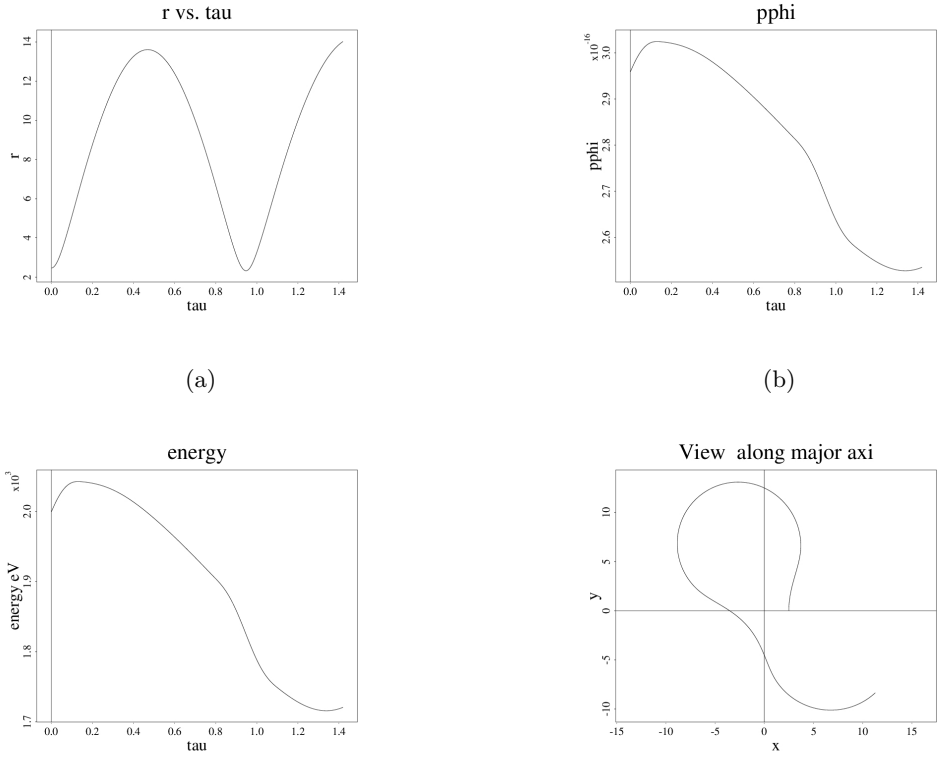

(a) (b)

(c) (d)

Figure 10: Single particle simulation result with rfac = 0.5, E0 = 2000

constraint on the escape factor as double the separatrix radius (2*7=14cm). Thus this sharp increase in confinement time corresponds to the particles at higher rfac having less maximum radial excursion, r_{max}: at a high enough rfac, particles' maximum radial excursion becomes less than the escape factor, thenceforth the particle stays confined with its regular betatron orbit.

This seems to suggest a trend where with the same initial angles, the bigger the initial r displacement, the smaller the r_{max}. Is this observed only when RMF heating is turned on? To investigate, I ran single particle simulations without RMF in the z=0 subspace, with E0 = 2000 eV. The results of the rfac and corresponding r_{max} are listed in Table 3. One can see that 1.4 is a

turning point. Before this rfac, r_{max} decreases with increasing rfac; after 1.4, r_{max} increases with increasing rfac. Particles started with rfac < 0.6 all escapes, meaning their r_{max} are greater than 14 cm, the escape line.

rfac	r_{max}/cm										
0.2	> 14	0.3	>14	0.4	>14	0.5	> 14	0.6	13.5	0.7	12.9
0.8	12.2	0.9	11.4	1.0	10.5	1.1	9.7	1.2	8.6	1.3	7.6
1.4	6.9	1.5	7.4	1.6	7.9	1.7	8.4				

Table 3: The single particle simulation results for initial conditions specified in Table 2, without RMF

This result in the z=0 subspace without RMF can be investigated analytically, since it can be reduced to a one-dimensional problem in r (Landsman thesis).

In the z=0 subspace, $A_\phi = \frac{B_0 r}{2}\left(1 - \frac{r^2}{r_s^2}\right)$, $p_z = z = 0$.

$$H = \frac{1}{2m}\left[(p_r)^2 + \left(\frac{p_\phi}{r} - \frac{q}{c}A_\phi\right)^2\right] = \frac{1}{2m}\left[(p_r)^2 + \left(\frac{p_\phi}{r} - \frac{qB_0 r}{2c}\left(1 - \frac{r^2}{r_s^2}\right)\right)^2\right] \tag{45}$$

$$= \frac{1}{2m}(p_r)^2 + \frac{1}{2m}\left(\frac{p_\phi}{r} - bR\rho\left(1-\rho^2\right)\right)^2 \tag{46}$$

$$= F(p_\rho^2 + (\frac{P}{\rho} - \rho(1-\rho^2))^2) \tag{47}$$

$$= F(p_\rho^2 - 2P + \frac{P^2}{\rho^2} + \rho^2(1+2P) - 2\rho^4 + \rho^6) \tag{48}$$

We then have equations of motion:

$$\dot{r} = \frac{\partial H}{\partial p_r} = \frac{\partial H}{\partial p_\rho}\frac{\partial p_\rho}{\partial p_r} = \frac{1}{bR}2Fp_\rho = \frac{bR}{m}p_\rho \tag{49}$$

$$\dot{\rho} = \frac{b}{m}p_\rho \tag{50}$$

$$\dot{p_r} = bR\dot{p_\rho} = Rm\ddot{\rho} = -\frac{\partial H}{\partial \rho}\frac{\partial \rho}{\partial r} = \frac{F}{R}(\frac{2P^2}{\rho^3} - 2\rho(1+2P) + 8\rho^3 - 6\rho^5) \tag{51}$$

$$\ddot{\rho} = \frac{2F}{R^2 m}(\frac{P^2}{\rho^3} - \rho(1+2P) + 4\rho^3 - 3\rho^5) = \frac{b^2}{m^2}(\frac{P^2}{\rho^3} - \rho(1+2P) + 4\rho^3 - 3\rho^5) \tag{52}$$

$$\ddot{\rho} = \frac{q^2 B_0^2}{m^2 c^2}(\frac{P^2}{\rho^3} - \rho(1+2P) + 4\rho^3 - 3\rho^5) \tag{53}$$

Equation (22) can be solved numerically to obtain the maximum r for each initial rfac, the results from this analytical treatment agrees with the simulation, as shown in Figure 4. The maximum r decreases as r increase from 0 to approximately 1.4; then, as r increases further, r_{max} increases. This change also corresponds to a sharp change where the initial rfac is the maximum or the minimum rfac. Thus, before the turning point, the class of orbit behaves such that the amplitude and frequency of oscillation in r decreases as rfac increases, and the decreasing rate is faster than the rfac increase. After the turning point, the frequency remains roughly similar while the amplitude increases.

The significance of rfac = 1.4 is that it gives a r close to $\sqrt{2} \times r_o = r_s \sim 1.41 \times r_o$. One may suspect, then, the separatrix somehow plays a big role in the orbit transition. However, zooming in further to the numerical solution, the turning point is not exactly at 1.41, instead it turns somewhere between $rfac \sim 1.37$. Single particle simulations are run to understand this transition as shown in Figure 5. The results suggest that the orbit becomes nearly a perfect circle around the turning point, which suggest that the value of critical rfac could be where perfect circular motion occurs.

$$F_c = \frac{mv^2}{r} = F_B = qvB_z = -qvB_0(1 - \frac{2r^2}{R^2}) \tag{54}$$

$$\frac{2r^3}{R^2} - r - \frac{mv}{qB_0} = 0 \tag{55}$$

Solving this polynomial in r gives $r_c = 0.0689$ cm, or rfac = 1.392, corresponding to the turning point. Thus, the particle's starting position is its maximum if it starts further than this critical r, because then the Lorentz force is stronger than the required circular motion centripetal force, and minimum if it starts inside this r because the Lorentz force is weaker than required centripetal force.

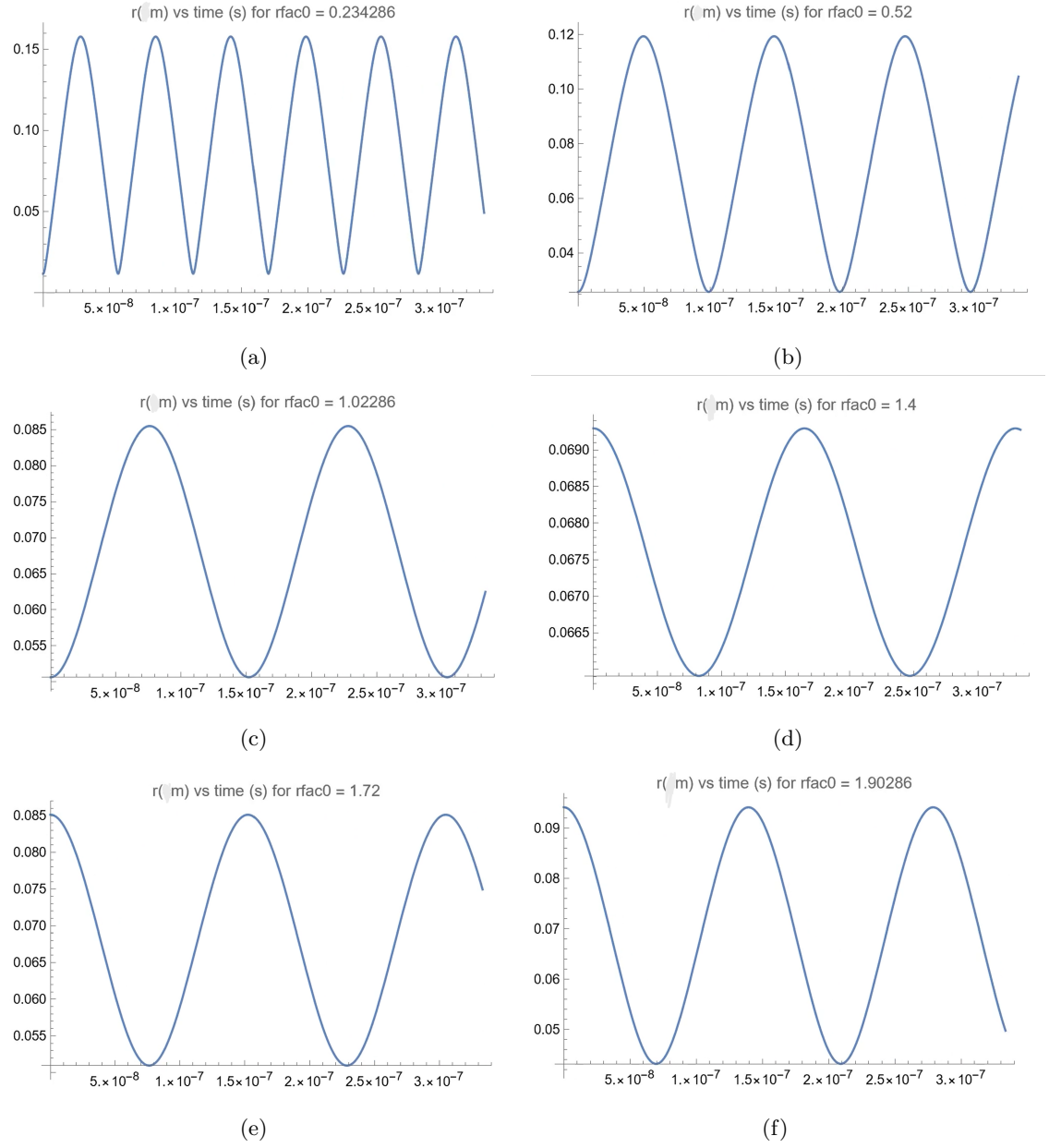

Figure 11: numerically evaluated results of r versus time for different initial rfac from differential equation of motion

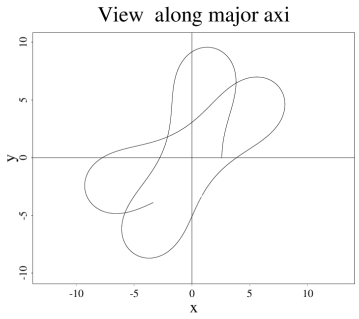

(a) rfac = 0.52

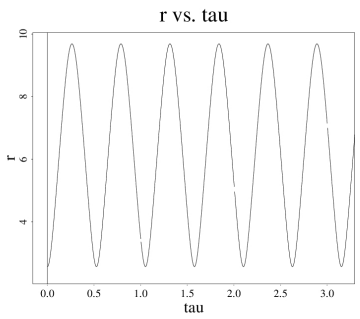

(b) rfac = 0.52

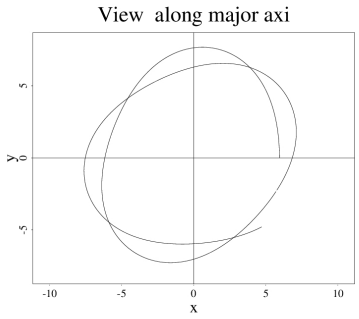

(c) rfac = 1.20

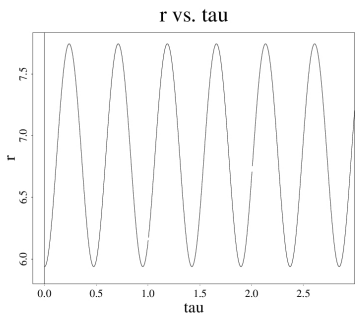

(d) rfac = 1.20

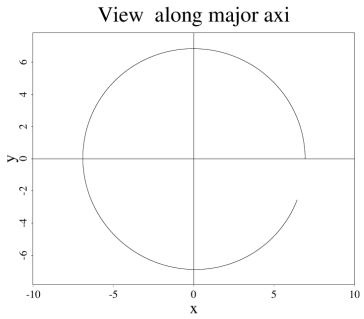

(e) rfac = 1.40

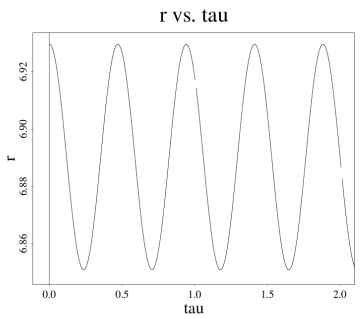

(f) rfac = 1.40

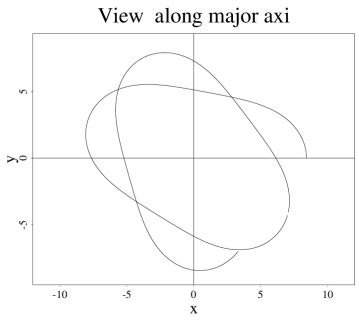

(g) rfac = 1.70

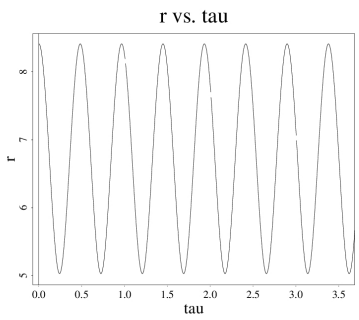

(h) rfac = 1.70

Figure 12: Single particle trajectories from RMF code simulation with Hill's vortex solution

4.1.2 Behaviours of particles with initial energy less than 2000eV in the z=0 subspace

parameters	values
omfac	1.1
b_0 (FRC)/G	1000
b_o (RMF)/G	10
r_s (FRC)/cm	7
κ (FRC)	2
ϕ_0	90
θ_0	90
z_{fac}	0
r_{fac}	0.1 - 1.7 (0.2, 8)
E_0 /eV	0 - 2000 (100, 20)
τ_{max}	5000

Table 4

What about particles with energies ranging from 0 to 2000 eV? Running the energy with 100eV step increase, from plots of Ebar and Emax against rfac in Figure 6 (a) and (e), we see that the maximum and average energy have similar trends: except for the particle where initial energy is zero, for any particle with $E0 > 100$ eV, the resultant heating does not depend on the initial rfac significantly. The initially static particle, however, gets heated only if the initial rfac is larger than 0.6, and heats to around 300 eV.

This trend can also be seen in the plot of Ebar and Emax against energy0, (b) and (f), where the lines of different rfac converges nicely except for a few, showing the lack of effect of initial rfac. Furthermore, the trend that the higher the initial energy, the higher the Ebar and Emax also generalizes to these lower energy particles. In the graphs we can see that the average energy follows the original energy very closely for rfac > 1 except for small energies ($\leqslant 100eV$) where significant heating occurs for rfac > 1. For small rfac (< 1) corresonding to the escaping orbits, there are more fluctuations in the energy, but generally still stays within 0.5 on the logarithmic scale of the original energy.

As for maximum energy, except for the escaping orbits which gains significantly more energy at maximum than original, and the small energy orbits ($\leqslant 100eV$) which heats up significantly beyond the o-point, all the other maximum energies stay close to the original energy.

The escape time trend generalizes nicely from last subsection: in the Escape time/rfac plot, we see that for particles with $E0 \leqslant 1000$ the confinement time for all rfac is approximately greater than or equal to 1000 tau. For particles with $E0 > 1500$ there are sharp cut offs in rfac beyond which the particles escape almost instantaneously. In general, the larger the initial energy, the narrower the range of stable rfac.

4.1.3 High energy ions (1500 - 2500 eV) beyond the the z=0 subspace

Do these conclusions still hold beyond the midplane? simulations are run with rfac = 1.2, zfac = 0, but $\theta_0 \neq 90$, meaning that the particle is no longer confined to the z=0 subspace. Energies are varied from 1500 to 2500 eV and θ_0 from 0 to 180. The results are shown in Figure 4.

This stable class of high energy ion orbits, which is observed to exist for high rfac (1.2 included) in the z=0 subspace, still exists beyond the z=0 subspace despite the particle not being confined to the midplane and potentially lost in the field line openings. This stability changes sharply depending on θ_0, analogous to the sharp jumping depending on rfac in the z=0 subspace. At around $\theta_0 = 90$, which is about the midplane, there exists a stable class of orbits; as energy increases, this band of stable orbits shrinks, as shown in (c) of Figure 6. This is qualitatively the same behaviour as observed in the rfac dependence in z=0 subspace: the higher the initial energy, the lower the band range of stable orbit parameters. The confinement time is much longer for this class of orbit ($\sim$ 3000 tau, compared to 0.6 tau of the escaping orbits).

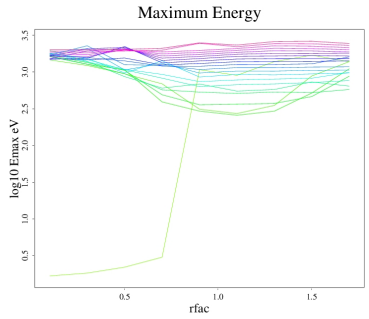

(a)

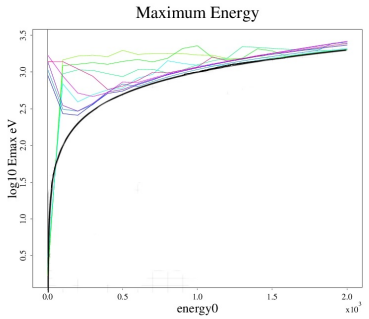

(b)

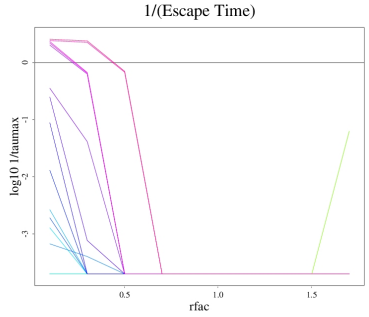

(c)

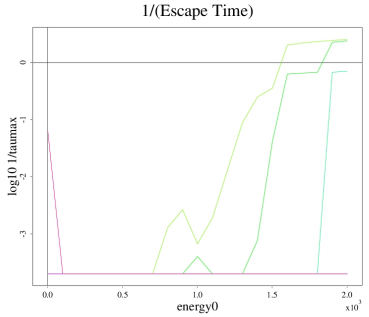

(d)

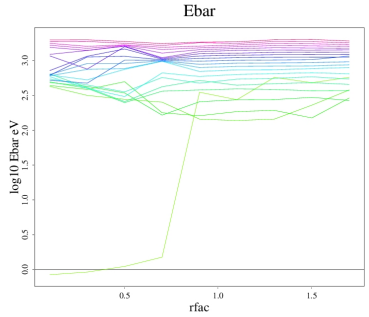

(e)

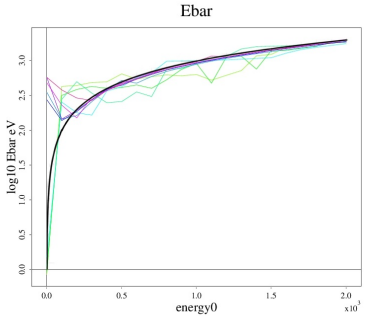

(f)

Figure 13: The black lines in (b) and (f) are the added identity lines showing the original energies

Despite the significant difference in the confinement time, the energy difference between the escaped and confined orbits are not significant. On average, the energy of the quickly escaping particles are higher than the stable ones, as shown in (e) of Figure 6. However, the energy difference between the stable and unstable orbits is not very significant (differ by $\sim$1.12 eV), compared to the confinement time difference (differ by $\sim$3000 tau). The stable high energy orbits are thus more preferable.

Overall the trend in average energy with respect to the initial energy still persists beyond the midplane. The higher the initial energy, the higher the average energy of the orbit and the energy changes are not significant. Most escaped particles gain energy on average and confined particles' bahaviours vary.

Where does the loss occur? Given the similar sharp confinement time change behaviour, are

parameters	values
omfac	1.1
b_0 (FRC)/G	1000
b_o (RMF)/G	10
r_s (FRC)/cm	7
κ (FRC)	2
ϕ_0	90
θ_0	0 - 180 (5, 36)
z_{fac}	0
r_{fac}	1.2
E_0 /eV	1500 - 2500 (100, 10)
τ_{max}	5000

Table 5

particles still lost through the side? Running single particle simulations, we see that the major loss occurs at the top and bottom field line openings due to the Zakkharov Vaccum field.

Thus the sharp decrease in confinement time as theta deviates from 90 degrees occurs when the z direction momentum is large enough so that the particle can reach the field line opening on top and bottom of the FRC. As the boundary is reached the particle suddenly starts getting lost; with a smaller z initial velocity the particle travels only in the region with closed field lines and do not get lost. Thus the significance of theta0 is that it gives the initial z direction momentum of the particle.

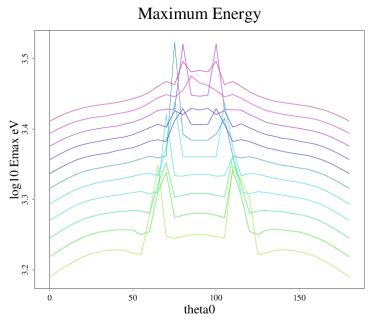

(a)

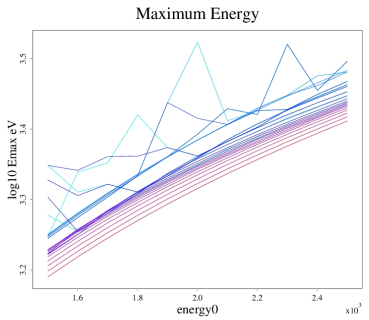

(b)

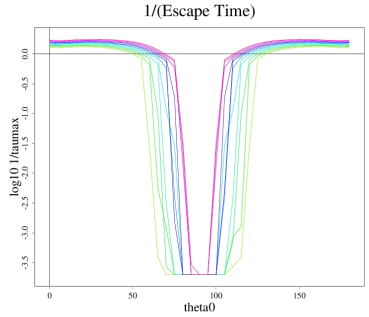

(c)

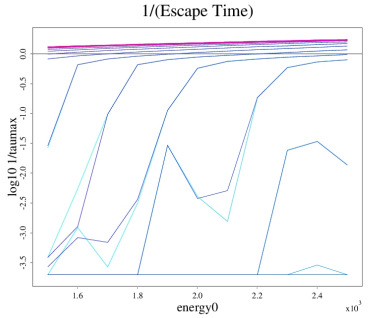

(d)

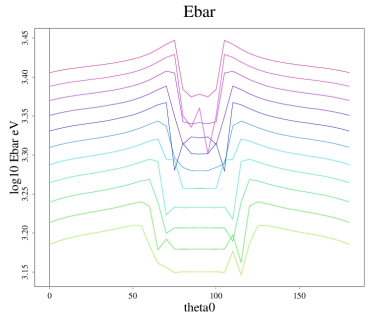

(e)

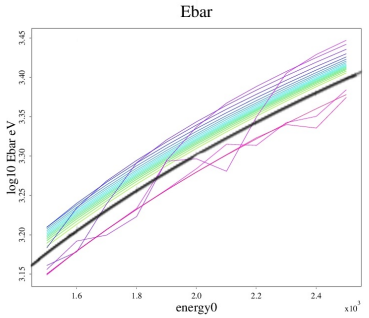

(f)

Figure 14: The black line in Ebar graph is the added identity line giving the initial energy in the logarithmic scale

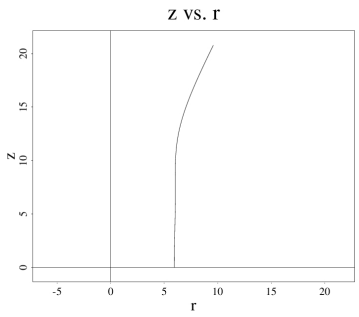

(a) theta0 = 30

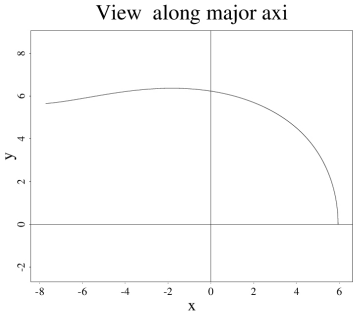

(b) theta0 = 30

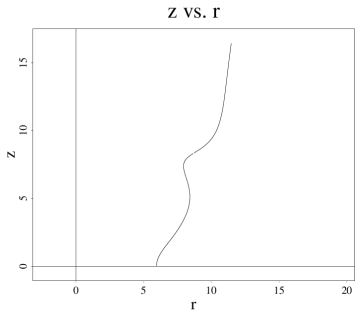

(c) theta0 = 70

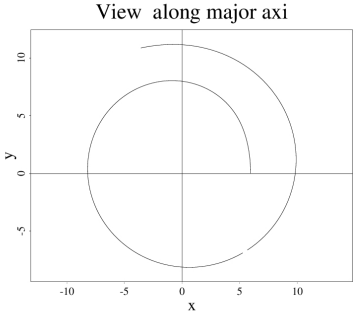

(d) theta0 = 70

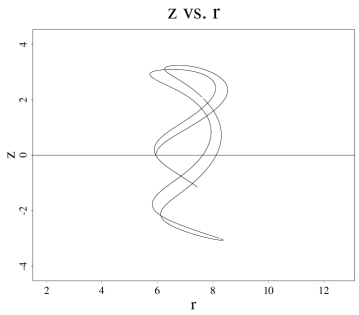

(e) theta0 = 80

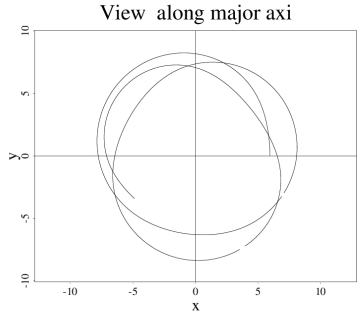

(f) theta0 = 80

Figure 15: Single particle trajectories in the z/r plane and the midplane for different theta0 and rfac = 1.2

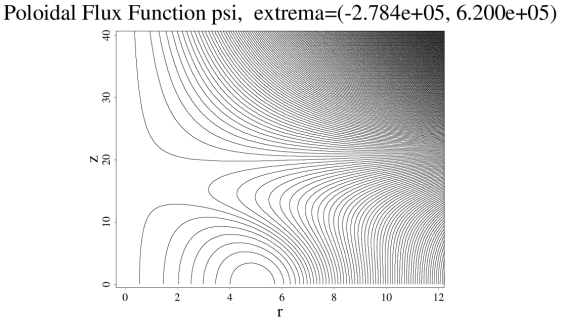

Figure 16: Magnetic field lines of the FRC with RMF enabling the Zakkharov Vaccum field

4.1.4 effects of rfac (initial r displacement) and theta0 (initial azimuthal angle) on 2000 eV ion

parameters	values
omfac	1.1
b_0 (FRC)/G	1000
b_o (RMF)/G	10
r_s (FRC)/cm	7
κ (FRC)	2
ϕ_0	90
θ_0	0 - 90 (5, 18)
z_{fac}	0 for Figure 8 and 0.1 for Figure 9
r_{fac}	0.1 - 1.7 (0.1, 16)
E_0 /eV	2000
τ_{max}	5000

Table 6

Outside the z=0 subspace, for a fixed rfac, the confinement depends sharply on the theta0. In the midplane, the confinement also depends sharply on the rfac. Is this still true outside the midplane? Two runs were done with different initial zfac varying theta0 and rfac, the results are shown in Figure 8 and 9. In the escape time versus theta0 and rfac plots in both figures, we see a sharp dependence on rfac and theta0.

From the Escape time versus theta0 plot (c) in Figure 9, we see particles outside the o-point radius (1 < rfac < 1.7) all show good confinement ($\sim 1000tau$) at theta0 > 85 degrees. Particles with rfac < 0.5 escape very quickly, for all angles. For rfac in between the particles only stay confined if it's very close to theta0=90. The Escape time versus rfac plot confirms this trend, showing that at larger rfac and close to 90 degrees theta0, particles are well-confined. This behaviour is not qualitatively affected by the initial zfac choice, as can be seen in Figure 10 (c) and (d).

As is the trend for rfac=1.2, for most rfac the average energy difference between the escaped and confined particles are not significant, making the well confined particles much preferable.

4.1.5 effects of a larger range of theta and rfac for E0 = 2000 eV for omfac = 1.5 and rs = 5 machine

parameters	values
omfac	1.5
b_0 (FRC)/G	1000
b_o (RMF)/G	10
r_s (FRC)/cm	5
κ (FRC)	2
ϕ_0	90
θ_0	-180 - 180 (20, 18)
z_{fac}	0
r_{fac}	0.1 - 1.7 (0.1, 16)
E_0 /eV	2000
τ_{max}	5000

Table 7

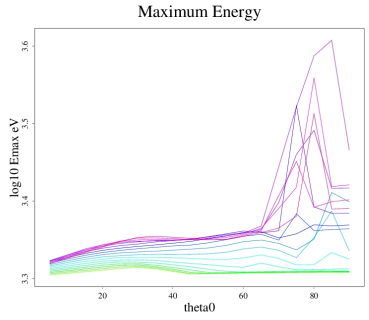

(a)

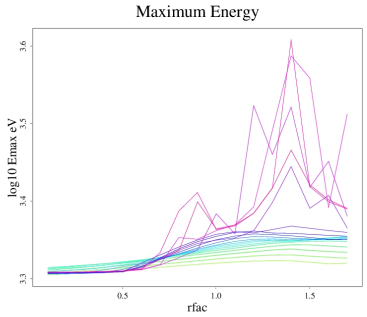

(b)

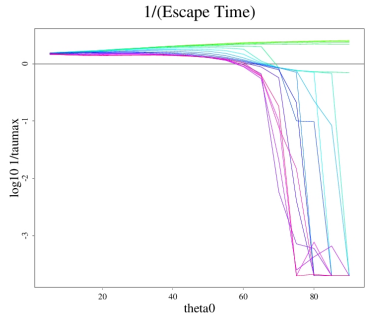

(c)

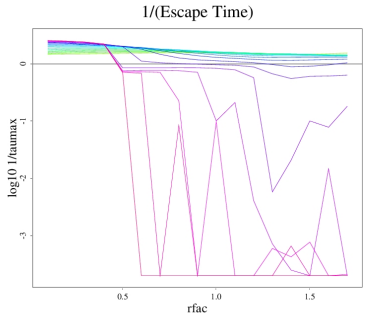

(d)

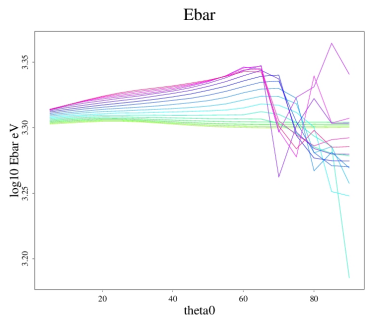

(e)

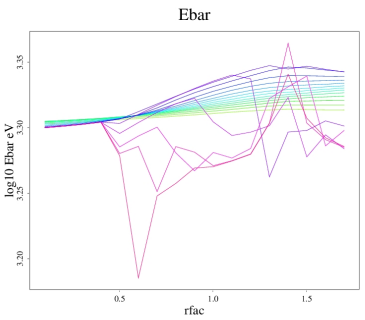

(f)

Figure 17: Plot of theta0 and rfac for zfac = 0 and E0 = 2000

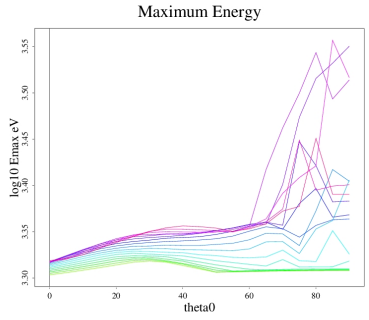

(a)

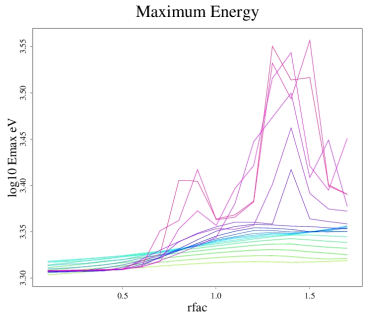

(b)

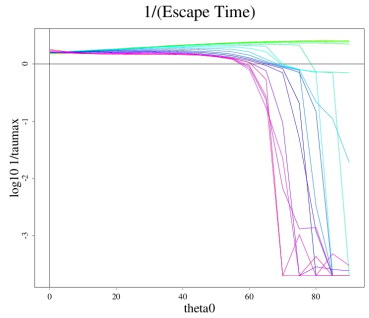

(c)

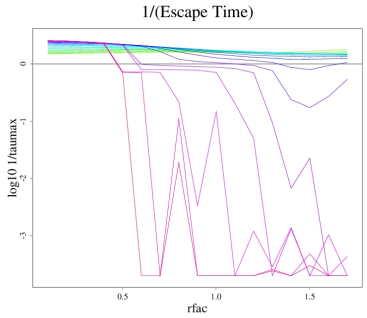

(d)

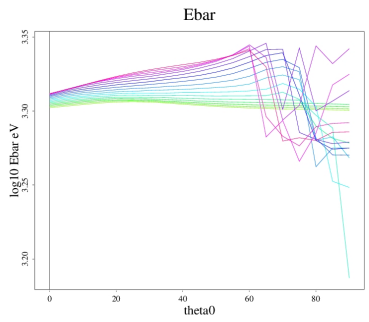

(e)

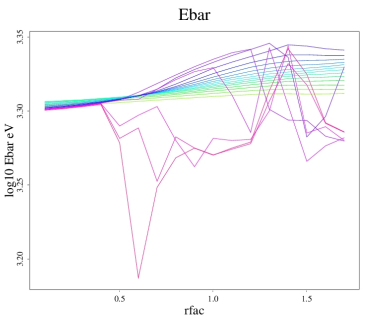

(f)

Figure 18: Plot of theta0 and rfac for zfac = 0.1 and E0 = 2000

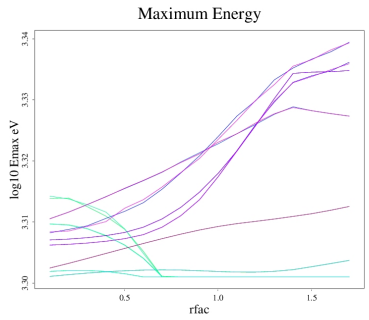

(a)

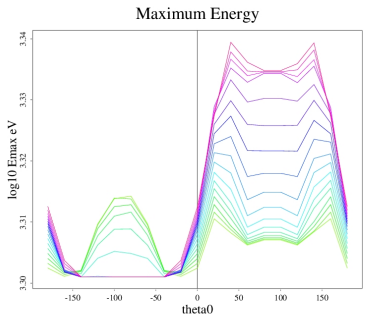

(b)

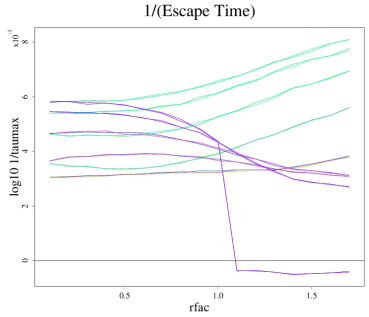

(c)

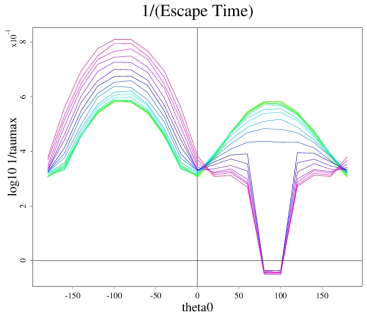

(d)

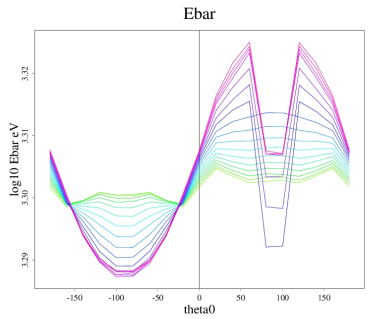

(e)

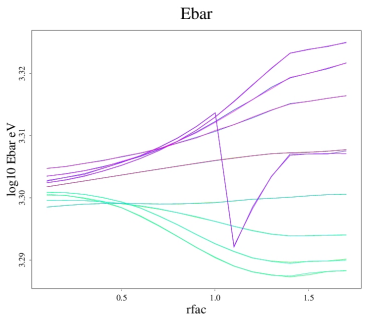

(f)

Figure 19: Plot of theta0 from -180 to 180 (step size 10) and rfac from 1 to 1.7 (step size 0.1) for zfac = 0, phi0 = 90, and E0 = 2000

For this simulation we switched to a different machine configuration with rs = 5 cm and omfac = 1.5. We also examined a larger span of initial theta0 from -180 to 180. The same conclusions follow that there exists a class of stable orbits around theta = 90 degrees which is around the midplane subspace. But the same stable orbit class do not exists for theta0 = -90 degrees. In general, particles shows poor confinement and heating when started with negative theta0. For positive theta0, larger rfac particles are heated better and better confined, but for negative theta0, the reverse is true. Plots of single particle trajectories are shown below, showing that poor confinement at negative theta0 to be due to the reversal of the initial velocity of the particle, thus the gyroradius being directed towards the separatrix.

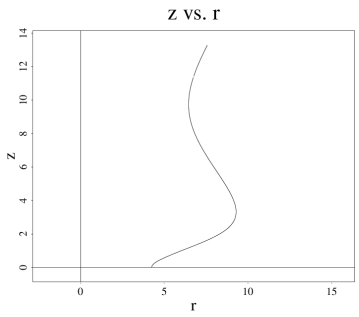

(a) theta0 = 80

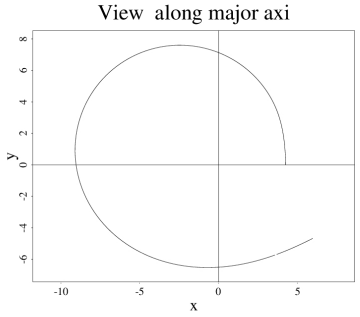

(b) theta0 = 80

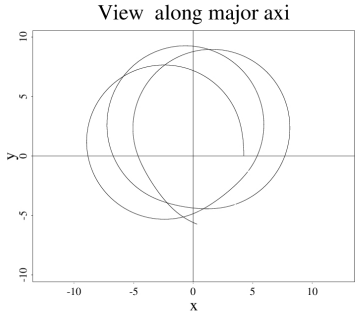

(c) theta0 = 88

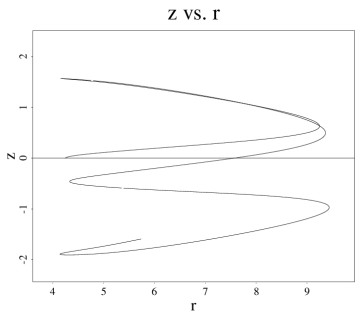

(d) theta0 = 88

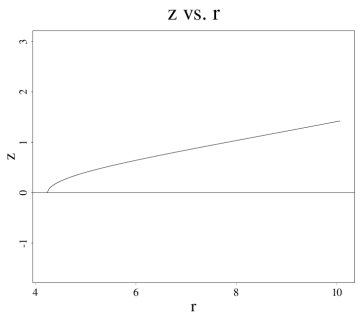

(e) theta0 = -80

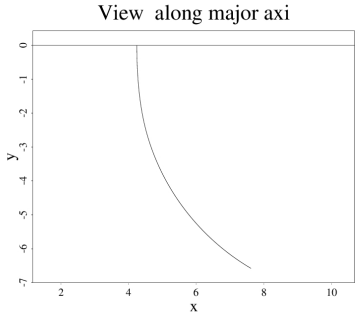

(f) theta0 = -80

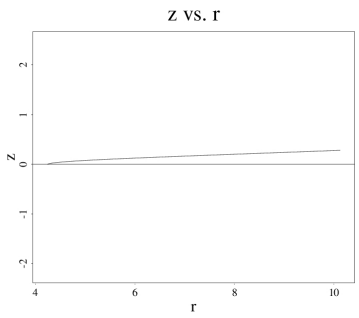

(g) theta0 = -88

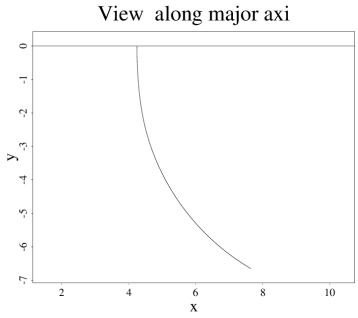

(h) theta0 = -88

Figure 20: Single particle trajectories of particles with positive and negative theta0 for rfac = 1.2, zfac = 0, phi0 = 90, and E0 = 2000

4.1.6 effects of theta0 on 2000eV particles with phi0 = 85 and zfac = 0.1

parameters	values
omfac	1.5
b_0 (FRC)/G	1000
b_o (RMF)/G	10
r_s (FRC)/cm	5
κ (FRC)	2
ϕ_0	85
θ_0	0 - 360
z_{fac}	0
r_{fac}	0.1 - 1.7 (0.1, 16)
E_0 /eV	2000
τ_{max}	5000

Table 8

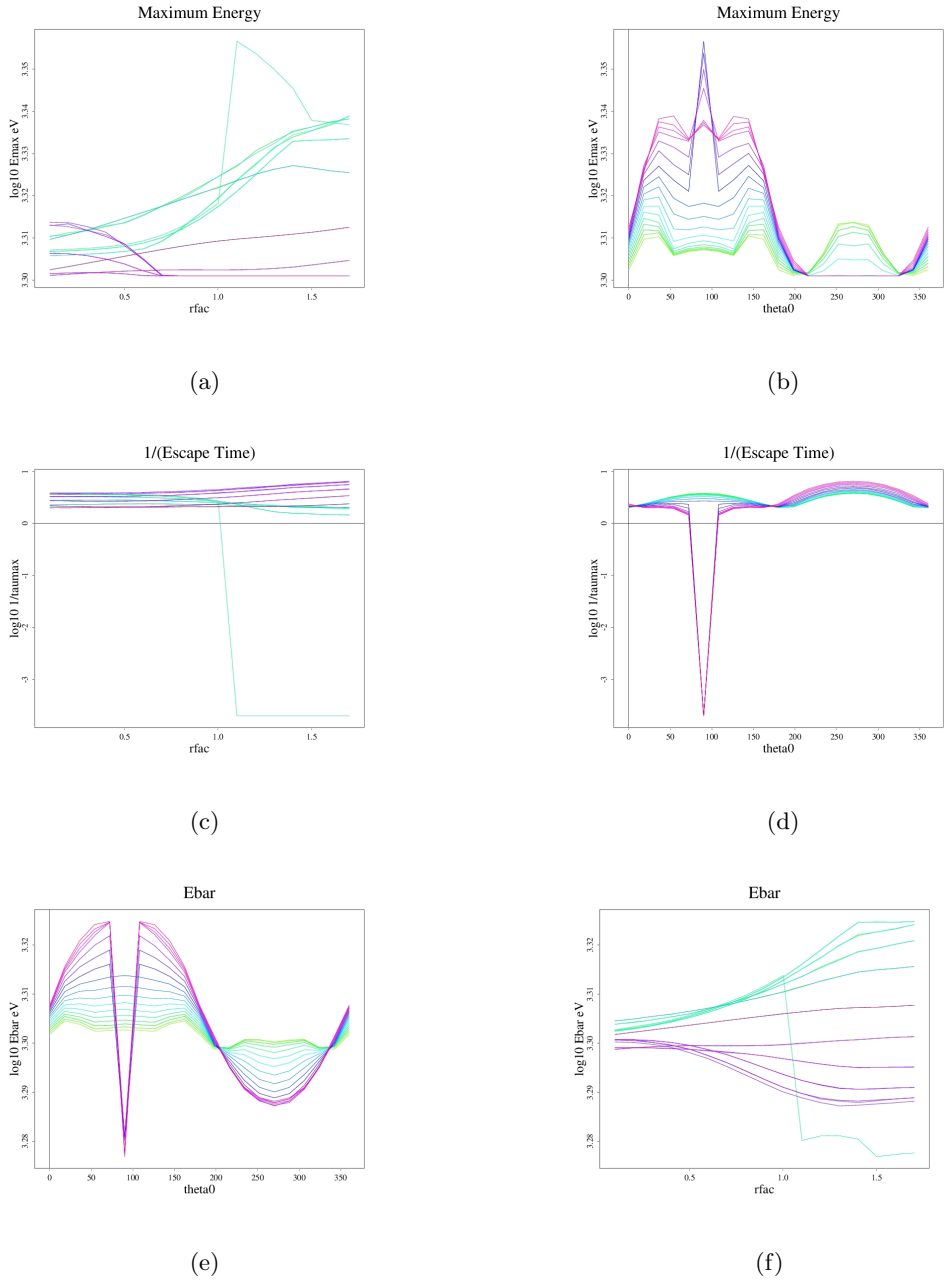

Figure 21: Plot of theta0 from 0 to 360 and rfac from 1 to 1.7 (step size 0.1) for zfac = 0, phi0 = 85, and E0 = 2

Changing the phi0 of the previous simulation to 85, the qualitative conclusions from the last subsection still follows. What about other initial phi0?

4.1.7 effects of phi0 on 2000eV particles

What effect does the initial phi0 have? Simulation suggests that at around phi0 = 90 - 110, there is a class of stable orbits with higher Emax and slightly lower average energy, which is what we worked with previously. However, if phi0 is set to other values, the confinement time is poor. This is again because of the alignment of the direction of gyration with the actual area inside the separatrix when phi0 is around 90.

parameters	values
omfac	1.5
b_0 (FRC)/G	1000
b_o (RMF)/G	10
r_s (FRC)/cm	5
κ (FRC)	2
ϕ_0	0 - 180 (10, 18)
θ_0	85
z_{fac}	0.1
r_{fac}	0.1 - 1.7 (0.1, 16)
E_0 /eV	2000
τ_{max}	5000

Table 9

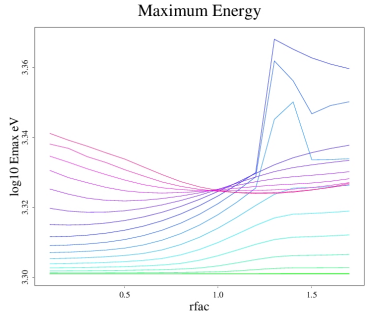

(a)

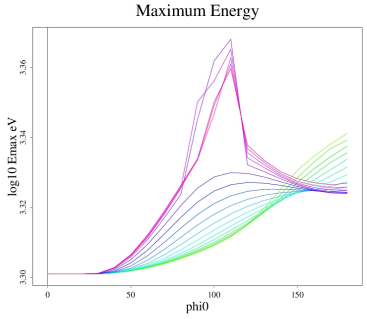

(b)

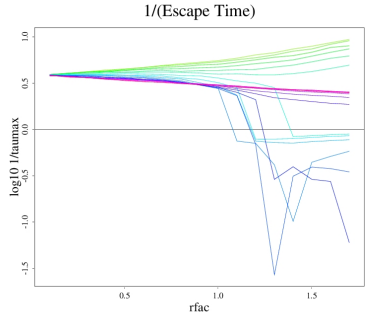

(c)

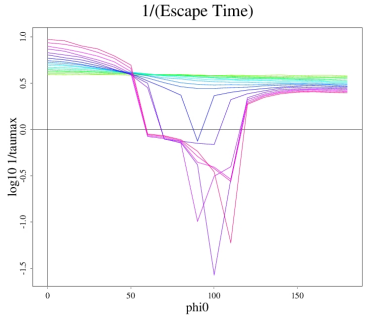

(d)

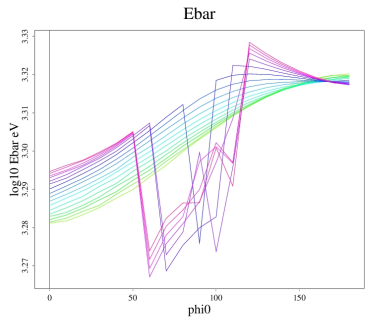

(e)

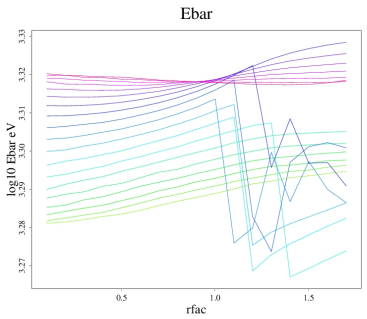

(f)

Figure 22: Plot of phi0 from 0 to 180 (step size 10) and rfac from 1 to 1.7 (step size 0.1) for zfac = 0.1, theta0 = 85, and E0 = 2

4.1.8 Behaviours of particles with initial energy less than 2000eV outside the mid-plane

parameters	values
omfac	1.1
b_0 (FRC)/G	1000
b_o (RMF)/G	10
r_s (FRC)/cm	7
κ (FRC)	2
ϕ_0	90 for F12 and F13; 130 for F14
θ_0	80 for F12; 90 for F13 and 14
z_{fac}	0.1
r_{fac}	0.1 - 1.7 (0.2, 8)
E_0 /eV	0 - 2000 (100, 20) for F13; 0 - 3000 (200, 15) for F12 and F14
τ_{max}	5000

Table 10

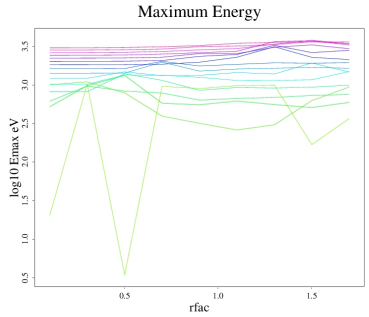

(a)

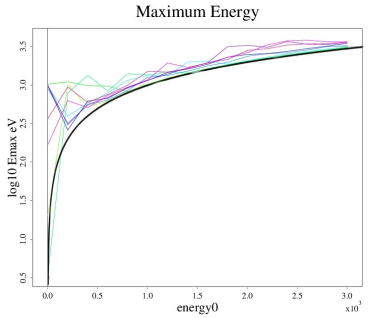

(b)

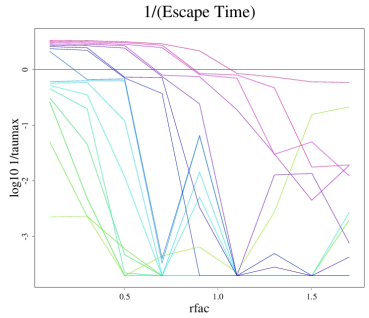

(c)

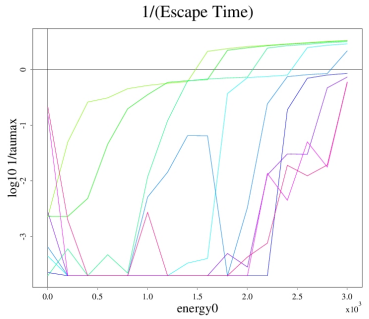

(d)

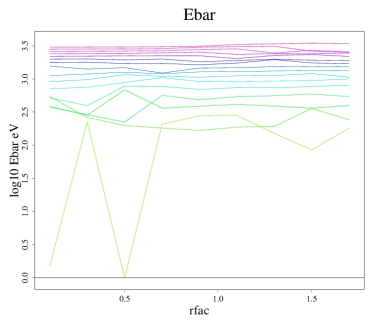

(e)

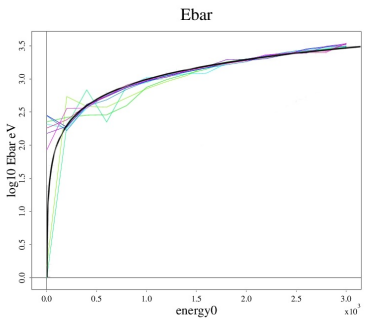

(f)

Figure 23: Plot of E0 and rfac for zfac = 0.1, phi0 = 130, and theta0 = 90

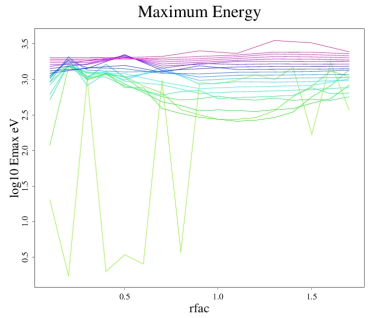

(a)

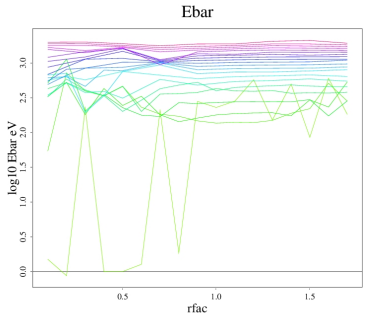

(b)

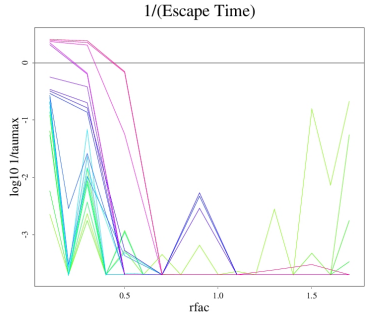

(c)

Figure 24: Plot of E0 and rfac for zfac = 0.1, phi0 = 90, and theta0 = 90

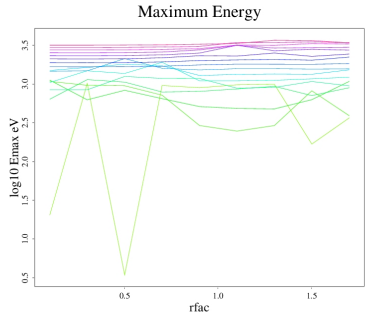

(a)

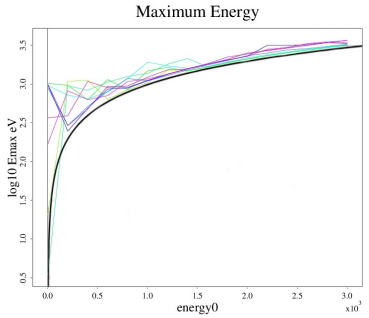

(b)

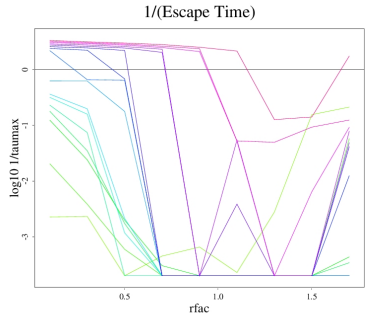

(c)

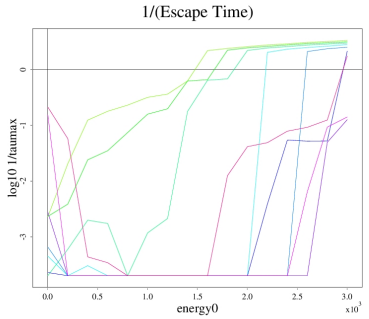

(d)

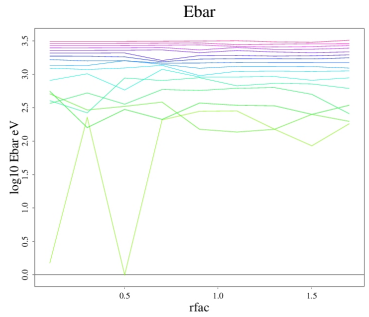

(e)

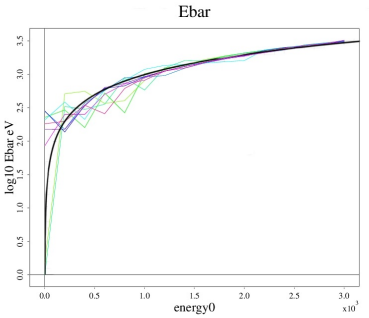

(f)

Figure 25: Plot of E0 and rfac for zfac = 0.1 and theta0 = 80

Three simulations outside of the midplane subspace were run with zfac=0, and different phi0 and theta0. Some trends are similar in these cases. The average energy and maximum energy are generally not significantly affected by rfac except for the small energy particles with $E0 < 500$ eV. Particles with lower energy generally shows better confinement at all these initial conditions, and particles started with larger rfac generally shows better confinement at each energy level, although there is not necessarily a sharp cutoff rfac above which particles are all stable for each energy.

The average energy generally stays very close to the starting energy in the timespan of 5000 tau, and is generally slightly below the original at around $E0 < 2000$ and above for $E0 > 2000$, except for small energy particles below 200 eV, which heats up significantly beyond $rfac \sim 0.5$. The maximum energy also stays close to the original, but generally slightly higher.

4.2 Low energy ions ($E0 \leqslant 200$ eV)

4.2.1 effects of initial energy from 0-40eV

parameters	values
omfac	1.1
b_0 (FRC)/G	1000
b_o (RMF)/G	10
r_s (FRC)/cm	7
κ (FRC)	2
ϕ_0	90
θ_0	90
z_{fac}	0.1
r_{fac}	0.1 - 1.6 (0.2, 8)
E_0 /eV	0 - 40 (2, 20)
τ_{max}	5000

Table 11

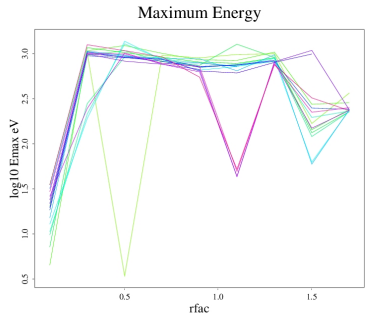

(a)

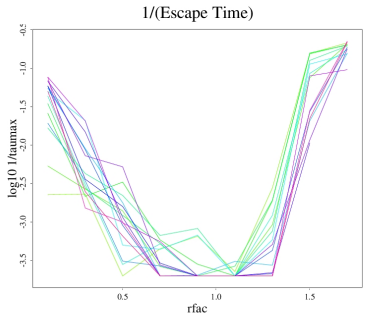

(b)

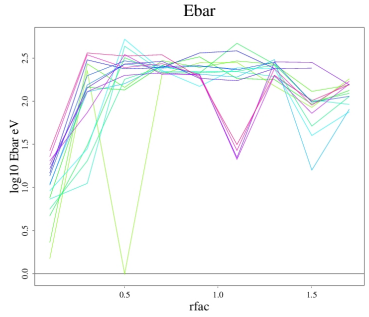

(c)

Figure 26: Plot of E0 from 0 to 40 (step size 2) and rfac from 1 to 1.6 (step size 0.2) for zfac = 0.1, phi0 = 90, and theta0 = 90

The particles in the range of 0 to 40 eV seems to behave similarly for the same initial conditions. The particles are the most stable around the o-point and escapes quickly if started beyond 1.5 and smaller than 0.3. Despite the difference in initial energy, the particles are heated similarly and have similar average energy of roughly 200 eV and maximum energy of around 1000 eV with some fluctuations.

4.2.2 effects of theta and rfac for E0 = 2 eV

parameters	values
omfac	1.1
b_0 (FRC)/G	1000
b_o (RMF)/G	10
r_s (FRC)/cm	7
κ (FRC)	2
ϕ_0	90
θ_0	0 - 90 (5, 18)
z_{fac}	0
r_{fac}	0.1 - 1.7 (0.1, 16)
E_0 /eV	2
τ_{max}	5000

Table 12

Now we focus specifically on particles with small initial energy of 2eV. Running two simulation examining the effects of rfac and theta0, for two different starting zfac (0 and 0.1), similar trends can be observed, suggesting that zfac is not a determining factor as long as not too large.

From plots with respect to theta0 in Figure 16 and 17, we see that the dependence on theta0 has no systematic trend, but undergoes random fluctuations and is overall horizontal. There is a stronger dependence of the particles' behaviours on rfac though; the particles all have a band of relative stability around the o-point (rfac = 1) and escapes quickly beyond rfac = 1.5 because of unclosed field lines. The maximum and average energy of the escaping particles are similar to and overall less than that of the better-confined particles, making these confined particles more desirable. There is also a dip in the energy at small rfac ($rfac < 0.2$), these particle is less well-confined and also does not get heated as well, they correspond to unstable cyclotron orbits.

The average energy of the well-confined particles are roughly level at around 100-300eV, and the maximum energy are at around 1000eV for all rfac between 0.3 and 1.4 and all theta0 except 90.

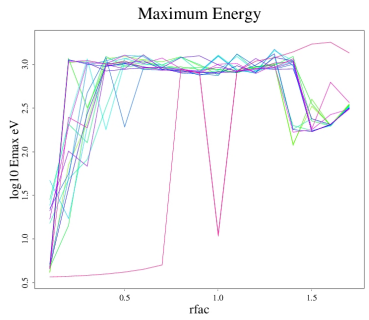

(a)

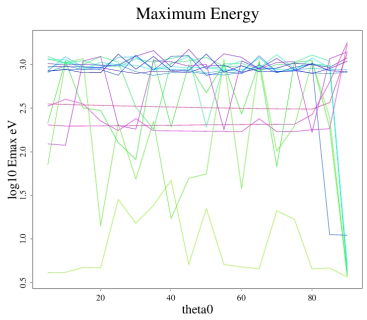

(b)

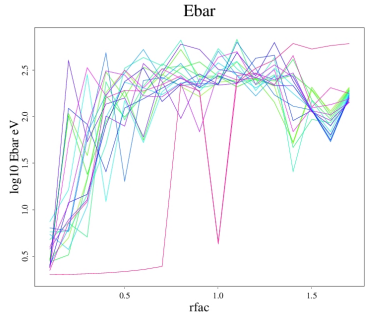

(c)

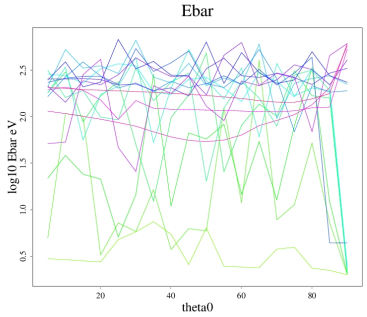

(d)

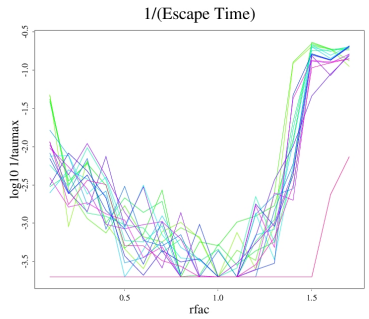

(e)

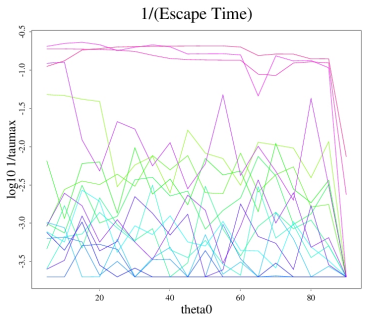

(f)

Figure 27: Plot of theta0 from 0 to 90 (step size 5) and rfac from 1 to 1.7 (step size 0.1) for zfac = 0, phi0 = 90, and E0 = 2

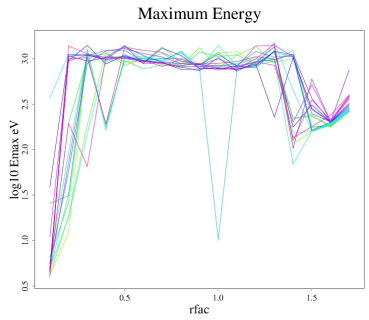

(a)

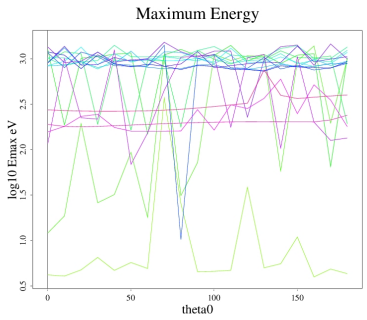

(b)

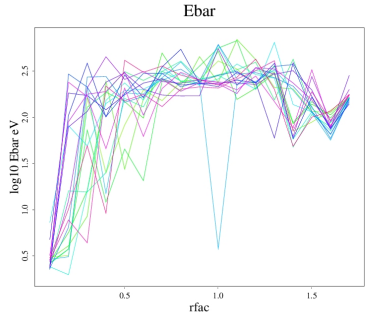

(c)

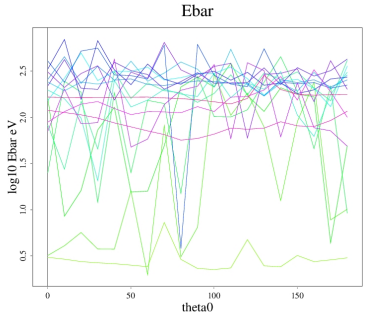

(d)

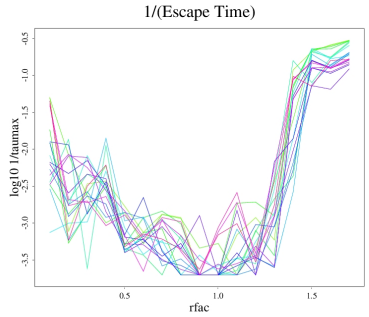

(e)

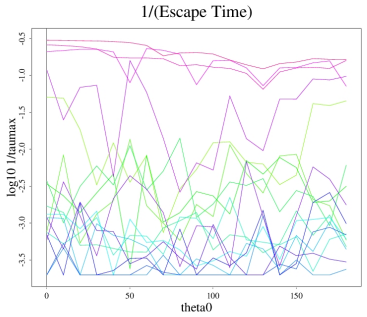

(f)

Figure 28: Plot of theta0 from 0 to 180 (step size 10) and rfac from 1 to 1.7 (step size 0.1) for zfac = 0.1, phi0 = 90, and E0 = 2

4.2.3 effectc of theta and rfac for E0 = 2 eV for omfac = 1.5 and rs = 5 machine

parameters	values
omfac	1.5
b_0 (FRC)/G	1000
b_o (RMF)/G	10
r_s (FRC)/cm	5
κ (FRC)	2
ϕ_0	90
θ_0	-180 - 180 (20, 18)
z_{fac}	0
r_{fac}	0.1 - 1.7 (0.1, 16)
E_0 /eV	2
τ_{max}	5000

Table 13

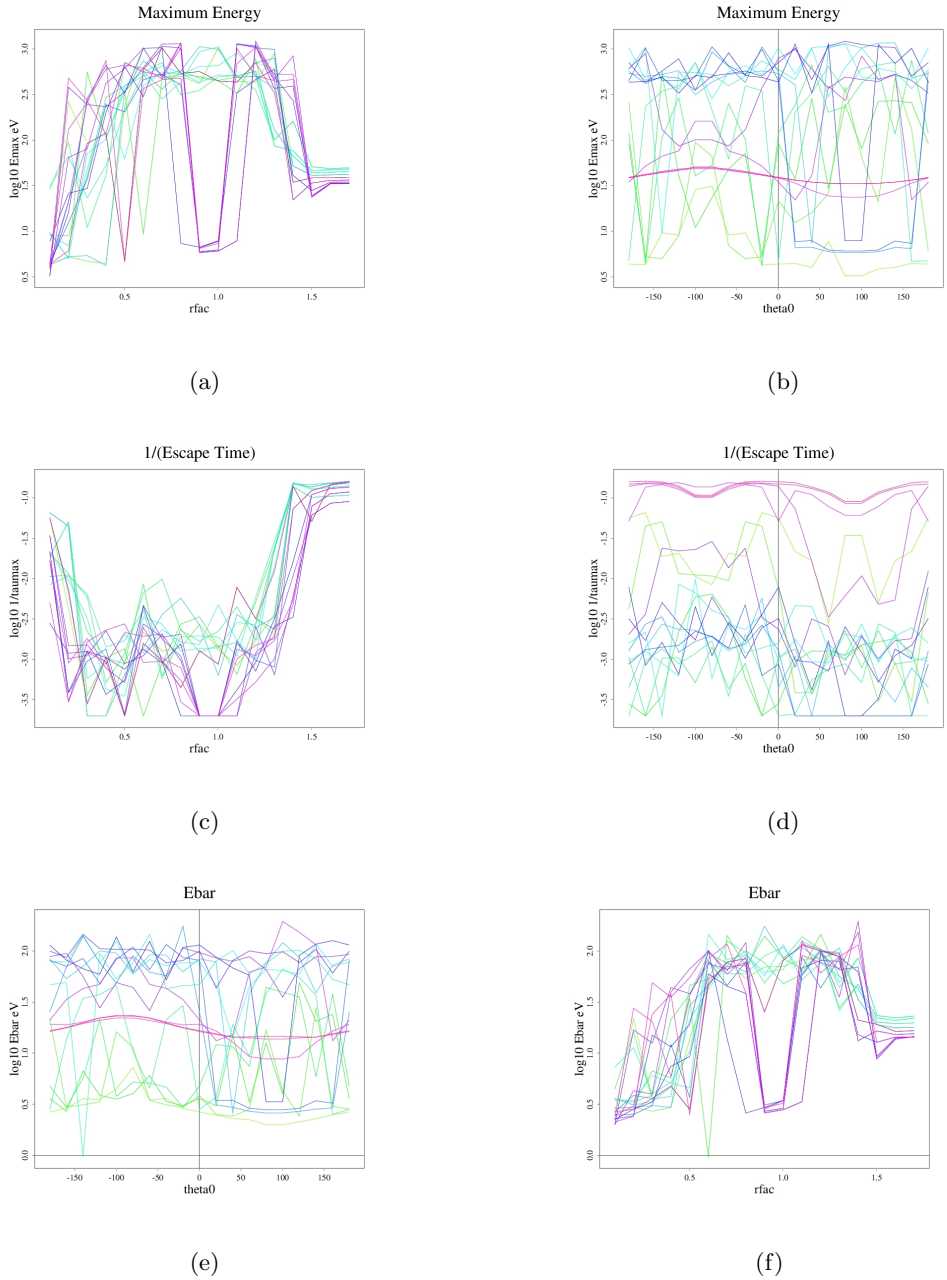

Figure 29: Plot of theta0 from -90 to 90 (step size 10) and rfac from 1 to 1.7 (step size 0.1) for zfac = 0, phi0 = 90, and E0 = 2

With a different machine configuration, the overall qualitative conclusions still follow, except for a very small class of orbits around the o-point which do not get heated.

4.2.4 optimal combination of omfac and bo

parameters	values
omfac	0.2 - 1.8 (0.1, 16) for 18; 0.4 - 1.6 (0.1, 12) for 20
b_0 (FRC)/G	1000
b_o (RMF)/G	0 - 20 (1, 20) for 18; 0 - 100 (5, 20) for 20
r_s (FRC)/cm	7
κ (FRC)	2
ϕ_0	90
θ_0	90
z_{fac}	0.1
r_{fac}	1.1
E_0 /eV	2
τ_{max}	5000

Table 14

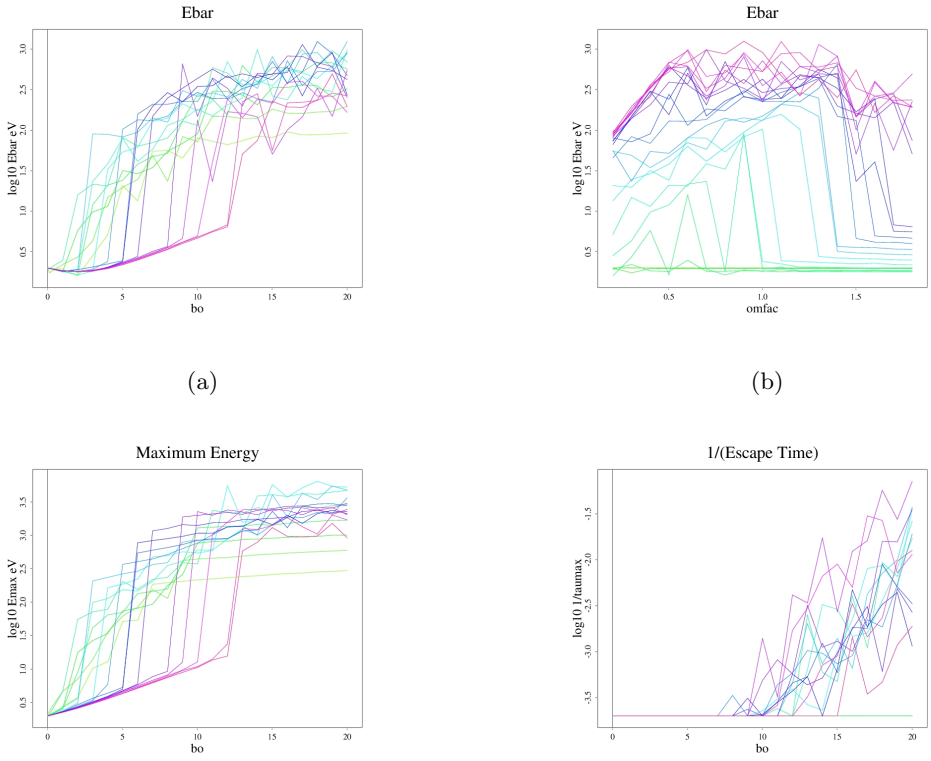

(a) (b)

(c) (d)

Figure 30: Plot of bo from 0 to 20 and omfac from 0.2 - 1.8 with phi0 = theta0 = 90, zfac = 0.1, rfac = 1.1, and E0 = 2 eV

The closer omfac is to 1, the more resonant the RMF is with the ion cyclotron frequency, hence the better the heating it and the worse the confinement time maybe. Same go for larger bo, giving better heating and worsening confinement. Therefore, to find an optimal confinement time and heating combination it is necessary to balance both omfac and bo. Running simulations on the heating of low energy ions (2 eV) with rfac =1.1 which belongs to the class of well confined particles examined in the last subsection.

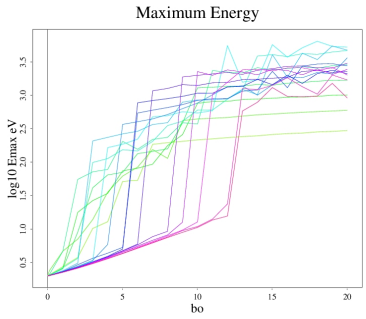

(a) E_{max} versus bo for omfac from 0.2 to 1.8 (0.1 step size)

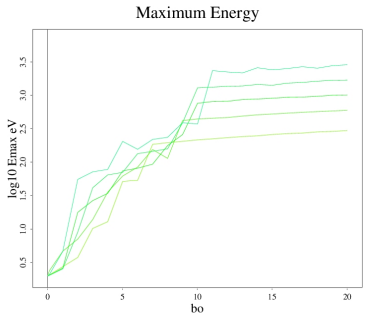

(b) omfac 0.2 - 0.6

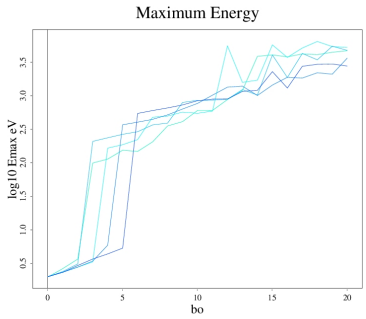

(c) omfac 0.7-1.1

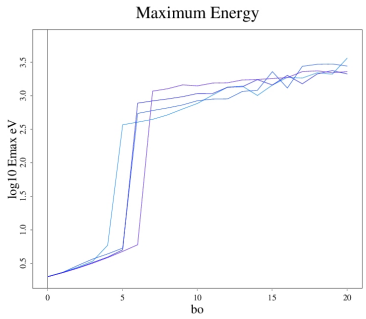

(d) omfac 1- 1.3

Figure 31: The detail of the Maximum energy again bo plot separating different curves representing different omfac

Looking at the graphs for maximum and average energy in Figure 18 (a) (c) and 19, one sees that, for omfac $\geqslant 0.7$ there is a sharp change from almost no heating to significant heating with Ebar $\sim$ 200 eV and Emax $\sim$ 1000 eV, this shape increase occurs at higher bo for higher omfac from 0.7 to 1.9. Beyond this critical value, increasing bo does not increase the heating significantly anymore. For smaller omfac from 0.2 to 0.6 there are more fluctuations and heating increases with bo from 0 to around 10, then it stays level despite increasing bo. Thus it is suggested that for a given omfac, it is fruitful to increase bo until the cutoff value, and any further increase in bo is less helpful.

Figure 18 (d) for the confinement time of particles suggest that the confinement time decrease with increasing bo, and bo = 10 G (bo/brfc ratio = 0.01) is a good value which gives confinement time over 1000 tau for all omfac, this value gives good heating for the particle we consider if omfac is anywhere between 0.2 and 1.5. To get even longer confinement time, one can use bo=5 (ratio = 0.005), and an omfac of 0.7-1 to get heating to $\sim$ 300eV max and $\sim$ 100 eV on average.

What about even larger bo/bfrc ratios? Does this behaviour extend qualitatively to large bo, and does increasing bo further does not bring any significant improvement in heating?

From Figure 20 (a) and (e), it is evident that beyond bo = 20 (ratio 0.02) there is really no change made to the heating by increasing bo any further; from (c) it is evident that for any bo beyond 20, the particles all quickly escape except for very small omfac $\leqslant 0.5$. Therefore, bo larger than 20 G when bfrc is 1000 G is really not desirable.

4.2.5 disparity between negative and positive omfac (5cm rs FRC)

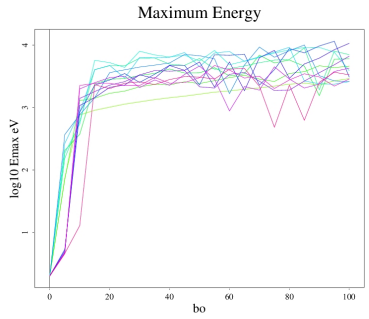

(a)

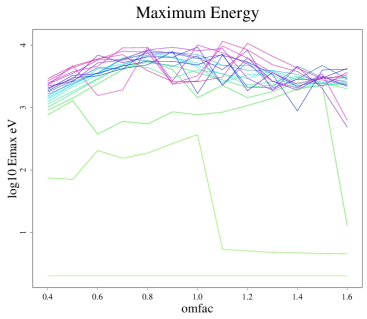

(b)

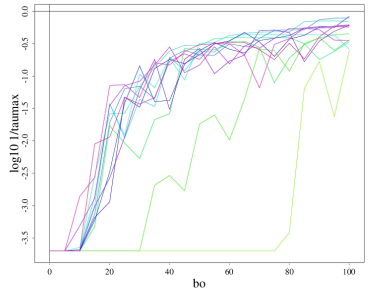

(c)

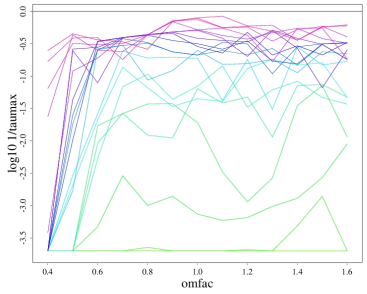

(d)

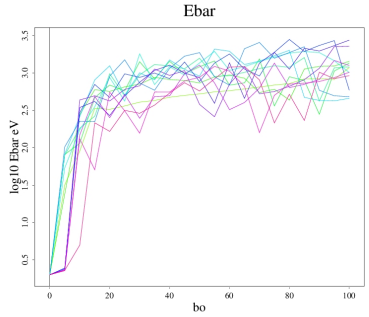

(e)

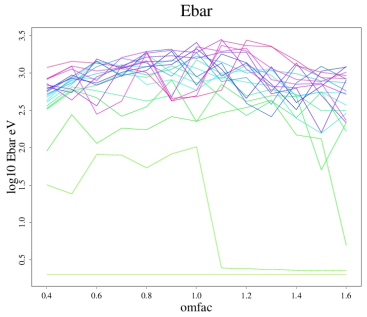

(f)

Figure 32: Plot of bo from 0 to 100 and omfac from 0.4 - 1.6 with phi0 = theta0 = 90, zfac = 0.1, rfac = 1.1, and E0 = 2 eV

But what about if we let the RMF rotate in the opposite angular direction as the ion cyclotron direction? Is there a symmetry?

This simulation suggests that at least for this particular orbit, the heating is not symmetrical with respect to the rotation direction of the RMF: when corotating in the same direction, the ion is heated better, also having a longer confinement time in general for almost all bo.

As bo is increased from 0, the maximum and average energy at each omfac increases, however, this increase

parameters	values
omfac	-2.2 - 2.2 (0.2, 22)
b_0 (FRC)/G	1000
b_o (RMF)/G	0 - 20 (2, 10)
r_s (FRC)/cm	5
κ (FRC)	2
ϕ_0	90
θ_0	90
z_{fac}	0.1
r_{fac}	1.2
E_0 /eV	2
τ_{max}	5000

Table 15

becomes negligible after bo reaches 10 G. This backs up our previous suggestion that 10 is a good number for bo (ratio of 0.01) providing good heating and good confinement time for all positive omfac. However, for negative omfac of around -0.4 there is a peak low of confinement time, for which bo = 10 also gives poor confinement. In this case $bo < 8$ gives better confinement.

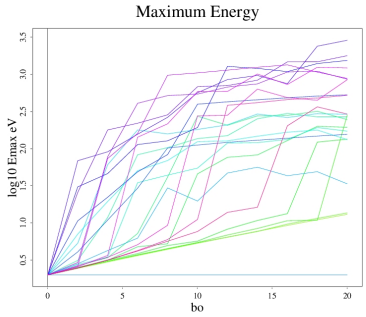

(a)

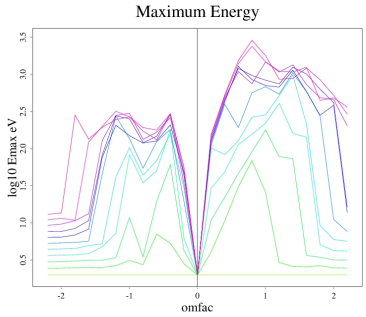

(b)

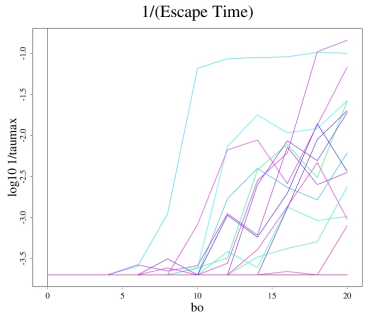

(c)

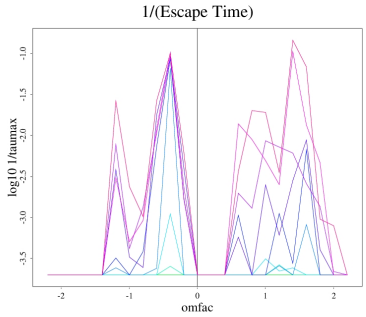

(d)

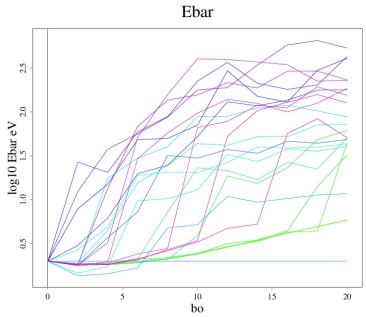

(e)

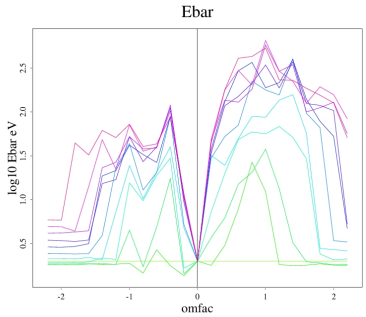

(f)

Figure 33: Plot of bo from 0 to 20 and omfac from -2.2 - 2,2 with phi0 = theta0 = 90, zfac = 0.1, rfac = 1.2, and E0 = 2 eV

4.2.6 effect of rs and omfac

parameters	values
omfac	-2 - 2 (0.2, 20)
b_0 (FRC)/G	1000
b_o (RMF)/G	10
r_s (FRC)/cm	3 - 8 (0.5, 10)
κ (FRC)	2
ϕ_0	90
θ_0	90
z_{fac}	0.1
r_{fac}	1.2
E_0 /eV	2
τ_{max}	5000

Table 16

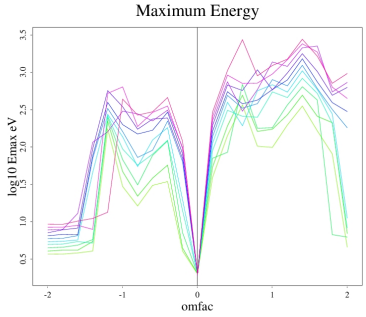

(a)

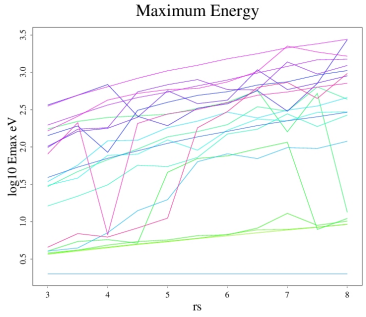

(b)

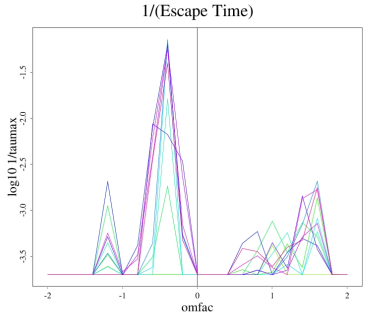

(c)

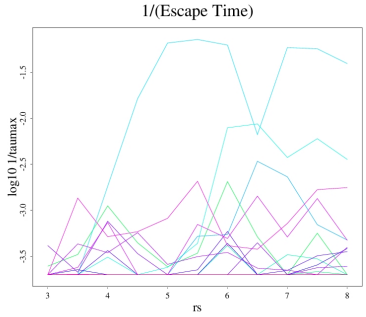

(d)

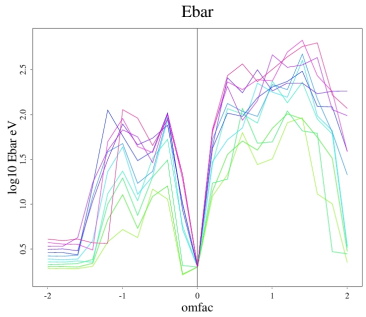

(e)

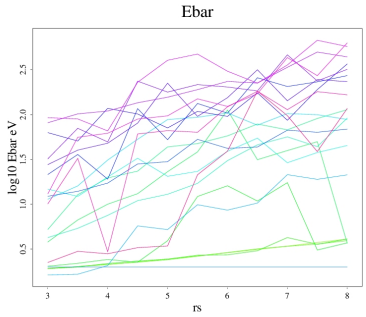

(f)

Figure 34: Plot of rs from 3 to 8 and omfac from -2 to 2 , with phi0 = theta0 = 90, zfac = 0.1, rfac = 1.2, and E0 = 2 eV

Fixing bo while varying rs does not qualitatively change the heating of particles; larger rs gives better heating with some random fluctuations.

4.2.7 effects of different components of induced electric field on heating

Magnetic field does no work, so the heating of particles are caused by the induced electric field from the RMF. Is there a component of the electric field which specifically contributes to the heating of the particles?

We first look t the z=0 subspace.

parameters	values
omfac	1.1
b_0 (FRC)/G	1000
b_o (RMF)/G	10
r_s (FRC)/cm	7
κ (FRC)	2
ϕ_0	90
θ_0	90
z_{fac}	0
r_{fac}	0.1 - 1.7 (0.1, 16)
E_0 /eV	2
τ_{max}	5000

Table 17

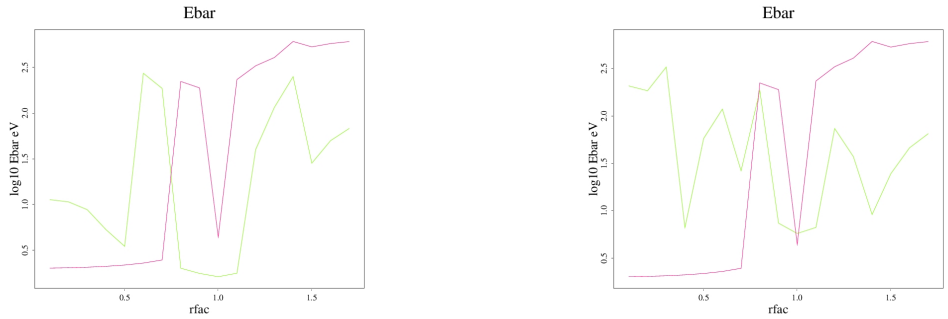

(a) $fudge_r$ (b) $fudge_\phi$

Figure 35: The red curve is the original data, while the green curve corresponds to the particle with the electric field in a certain direction turned off

There is no vector potential, hence no electric field in the z direction in the midplane, so it has no effect on the heating. Turning off the r direction and phi direction electric field in Figure 21, we see that in regions where there were originally no heating, turning off the phi direction electric could cause there to be more heating for rfac $\leqslant$ 0.5, and turning off the r-direction electric field could results in heating for rfac between 0.5 and 0.6. Meanwhile, for particles which are originally heated, the heating gets worse than original if either of the r or phi direction electric field are turned off. This suggests that the lack of heating for small rfac maybe due to the regular interaction of the cyclotron orbit with the induced electric field, while turning off one of the components disrupts this regular interaction, resulting in better heating. Meanwhile, both r and phi direction electric field contributes to the heating for particles originally heated in the midplane.

Outside the midplane, what can be said?

parameters	values
omfac	1.1
b_0 (FRC)/G	1000
b_o (RMF)/G	10
r_s (FRC)/cm	7
κ (FRC)	2
ϕ_0	90
θ_0	90
z_{fac}	0.1
r_{fac}	0.1 - 1.7 (0.1, 16)
E_0 /eV	2
τ_{max}	5000

Table 18

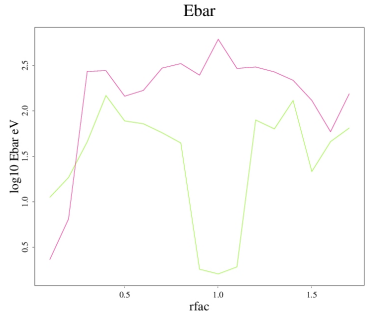

(a) $fudge_r$

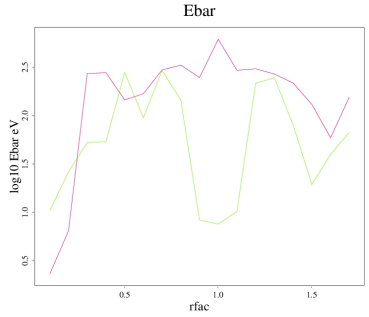

(b) $fudge_\phi$

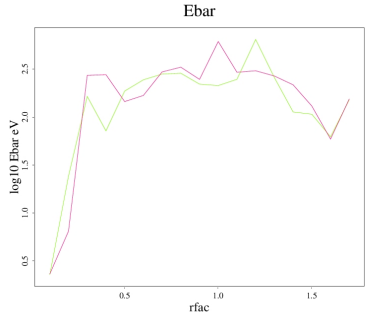

(c) $fudge_z$

Figure 36: The red curve is the original data, while the green curve corresponds to the particle with the electric field in a certain direction turned off

Beyond the midplane, we see similarly that particles which originally do not get heated (at $\sim$ 0.1 = rfac) could become better heated if one of the r or ϕ component of the electric field is turned off. For a particle that's originally heated to around 200 eV, turning off either component could reduce the heating to none around the o-point and could lead to a decrease by around 100 eV elsewhere. On the other hand, the z component of the electric field plays no role in the overall heating of the particle.

4.2.8 effects of different components of induced electric field on heating with different a FRC and RMF

parameters	values
omfac	1.5
b_0 (FRC)/G	1000
b_o (RMF)/G	10
r_s (FRC)/cm	5
κ (FRC)	2
ϕ_0	90
θ_0	90
z_{fac}	0.1
r_{fac}	0.1 - 1.7 (0.1, 16)
E_0 /eV	2
τ_{max}	5000

Table 19

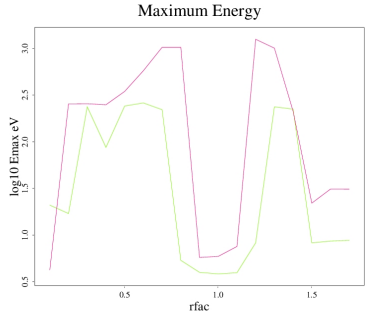

(a) $fudge_r$

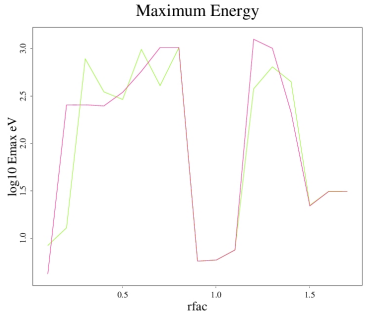

(b) $fudge_z$

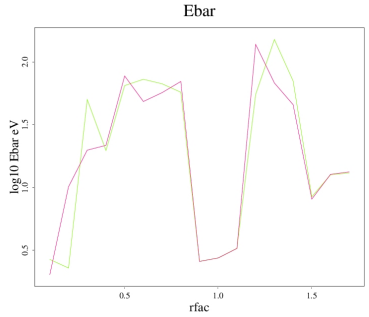

(c) $fudge_z$

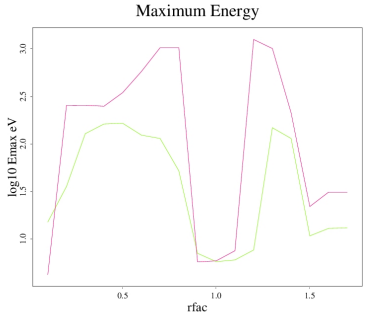

(d) $fudge_\phi$

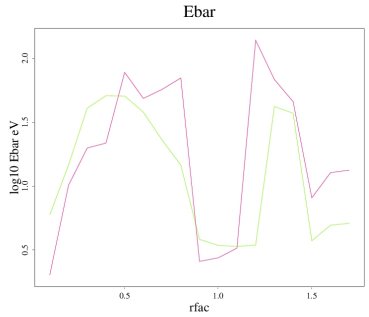

(e) $fudge_\phi$

Figure 37: The red curve is the original data, while the green curve corresponds to the particle with the electric field in a certain direction turned off

parameters	values
omfac	1.5
b_0 (FRC)/G	1000
b_o (RMF)/G	10
r_s (FRC)/cm	5
κ (FRC)	2
ϕ_0	90
θ_0	80
z_{fac}	0
r_{fac}	0.1 - 1.7 (0.1, 16)
E_0 /eV	2
τ_{max}	5000

Table 20

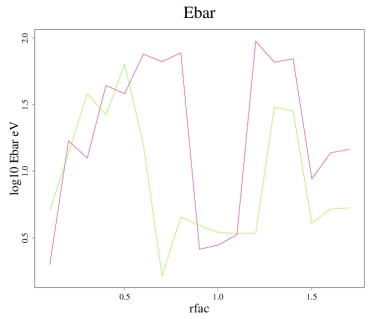

(a) $fudge_\phi$

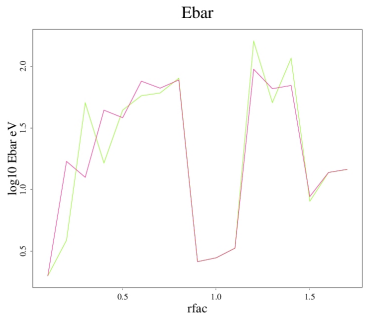

(b) $fudge_z$

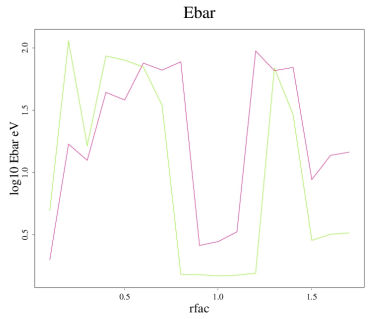

(c) $fudge_r$

Figure 38: The red curve is the original data, while the green curve corresponds to the particle with the electric field in a certain direction turned off

Running the simulations for two different starting conditions for theta0 and zfac in a FRC with rs = 5cm and RMF with omfac = 1.5, we see that beyond the subspace and with a different geometry some conclusions still seem to generalize: both the r and ϕ components contribute to the heating of a low energy ion somewhat equally, while the z component does not contribute to the heating.

4.2.9 effects of different components of the electric field on higher energy particles (2000 eV)

parameters	values
omfac	1.5
b_0 (FRC)/G	1000
b_o (RMF)/G	10
r_s (FRC)/cm	5
κ (FRC)	2
ϕ_0	90
θ_0	80
z_{fac}	0
r_{fac}	0.1 - 1.7 (0.1, 16)
E_0 /eV	2000
τ_{max}	5000

Table 21

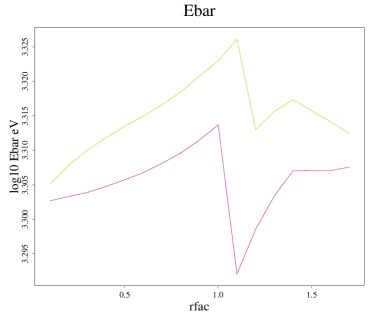

(a) $fudge_r$

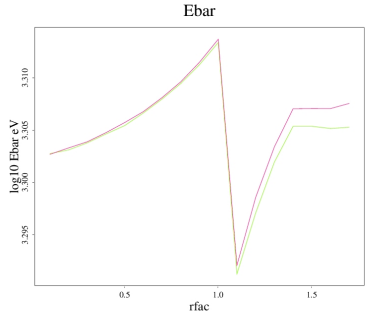

(b) $fudge_z$

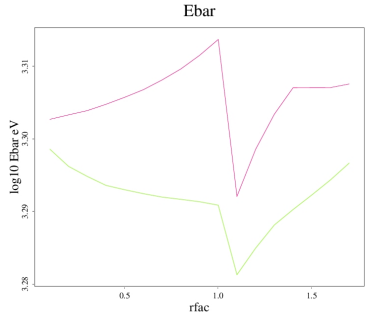

(c) $fudge_\phi$

Figure 39: The red curve is the original data, while the green curve corresponds to the particle with the electric field in a certain direction turned off

For high energy particles, turning off the r direction electric field seems to increase the heating by roughly 100 eV, and turning off the ϕ electric field decreases the heating by roughly 50 - 100 eV.

4.2.10 effects of phi0

parameters	values
omfac	1.1
b_0 (FRC)/G	1000
b_o (RMF)/G	10
r_s (FRC)/cm	5
κ (FRC)	2
ϕ_0	0 - 360 (20, 18)
θ_0	90
z_{fac}	0.1
r_{fac}	0.1 - 1.7 (0.1, 16)
E_0 /eV	2
τ_{max}	5000

Table 22

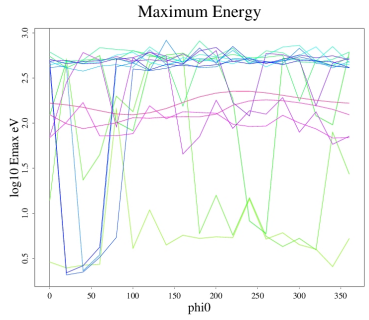

(a)

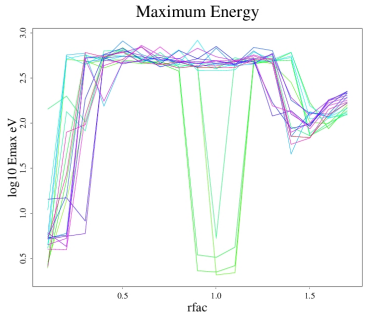

(b)

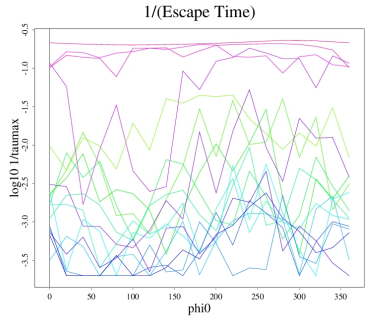

(c)

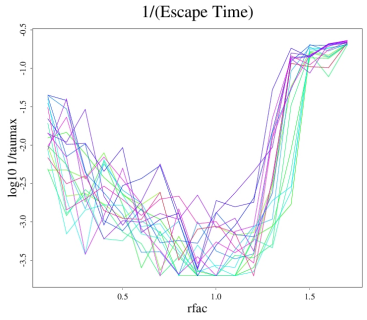

(d)

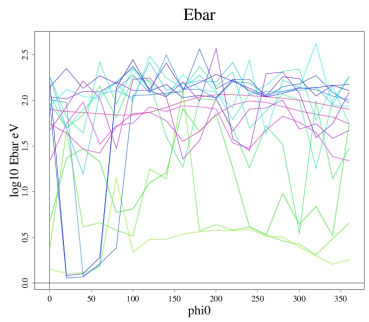

(e)

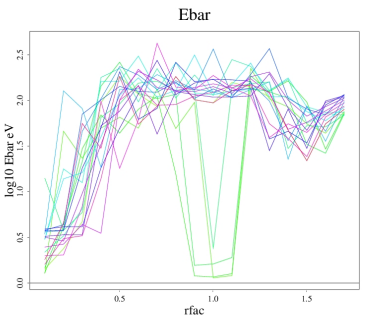

(f)

Figure 40: The effects of varying phi0 for a 2 eV ion not in the midplane

From Figure 26 (b) (d) and (f) we see that the effect of phi0 causes almost random variations in the original trend. However, it is still true overall that the confinement time is good around the o-point and less so beyond rfac = 1.5 or smaller than 0.3. The maximum energy and average energy are also not significantly changed by phi0, except for a very small band of particles around phi0=50 and rfac=1 which do not get heated.

5 Conclusion

In this report we discussed the importance of gyroradius in the particle not following its original closed field line and escaping in Section 2.

A mechanism for gaining net z momentum is proposed in Section 3, where a spike in energy occurring at the right time can result in a net positive or negative z impulse imparted on the particle, resulting in fluctuating z oscillation amplitude and thus the loss of the particle through the field line openings.

For high enegry particles, in the z=0 subspace, we find that there is a sharp dependence of the escape time on rfac at a given energy from 1300 to 3300 eV, where particles are well confined at larger rfac, and this band of stability is larger for smaller energy. Smaller energy particles with E0 less than 1000 eV have confinement time greater or equal to aorund 1000 tau. Particles are lost from the side and the maximum r excursion of the orbits decrease for increasing rfac until a critical rfac around 1.4 where the particle orbit becomes a circle around the z axis. Small energy orbits with energy less than 100 eV heats up to a few hundred eV if started beyond the o-point. And for any particles with energy larger than that, the average and maximum energy stays close to the original energy for the duration of 5000 tau, particles with energy0 larger than 2500 could gain energy but losses energy otherwise.

Beyond the midplane, for both machine configurations we see that for particles with energy from 1500 to 2500 eV, phi0 = 90, and rfac = 1.2, there is a sharp dependence of the confinement time on the theta0, giving a band of stable orbit at around theta = 90 degrees, which is wider at lower energy. This class of stable orbits has similar energy as the lost orbits and are thus more desirable. The lost mechanism in this case is through larger pz at larger theta0, resulting in particles reaching open field lines and thus getting lost. For the particles which are in the relatively stable class, the confinement also depends sharply on rfac, with particles at larger rfac being more stable. Particles outside the o-point all shows confinement of around 1000 tau at theta between 85 and 90 degrees. Particles with rfac less than 0.5 escape very quickly for all angles. The average energy stays close to the initial energy and goes slightly higher for E0 greater than 2000 eV and lower for E0 less than that, except for small energy particles with energy less than 200 eV, which heats up significantly beyond rfac of around 0.5. For other initial phi0 not in the range of 90 - 110 the particle is poorly confined because of the particle trajectory crossing the escape line.

For low energy particles, the behaviours are similar for E0 from 0 to 40 eV with phi0 = 90 for both machines. There is a relatively stable class of orbits which is also heated up, around the o-point and all particles escape quickly if started beyond the separatrix or at less than 0.5 rfac. There is no systematic dependence on theta0 for low energy particles. The average energy of relatively well-confined particles are around 100-300eV and maximum energy around 1000 eV.

Increasing bo generally increases the heating. For a 2eV ion, at each omfac there is a sharp increase from almost no heating to heating at a critical bo value between 0 and 15 G. Beyond this critical value, increasing the bo doesn't increase the heating significantly but decreases the confinement time. bo = 10 G or a ratio of 0.01 gives confinement over 1000 tau for all omfac and gives good heating is omfac is anywhere between 0.2 and 1.5. There is an asymmetry between positive and negative omfac, with positive omfac giving better heating and confinement. Larger rs gives better heating and phi0 doesn't have a systematic effect for low energy particles.

The z direction electric field has almost no effect in the heating of the particles, and the r and phi direction fields plays equally important roles.

References

[1] S. A. Cohen, A. S. Landsman, and A. H. Glasser. Stochastic ion heating in a field-reversed configuration geometry by rotating magnetic fields. *Physics of Plasmas*, 14(7):072508, 2007.

[2] S. A. Cohen and R. D. Milroy. Maintaining the closed magnetic-field-line topology of a field-reversed configuration with the addition of static transverse magnetic fields. *Physics of Plasmas*, 7(6):2539–2545, 2000.

[3] A. S. Landsman, S. A. Cohen, and A. H. Glasser. Regular and stochastic orbits of ions in a highly prolate field-reversed configuration. *Physics of Plasmas*, 11(3):947–957, 2004.

[4] A. S. Landsman, S. A. Cohen, and A. H. Glasser. Onset and saturation of ion heating by odd-parity rotating magnetic fields in a field-reversed configuration. *Physical Review Letters*, 96(1), 2006.

6 Terminology

Ebar/$\overline{E}$	average energy	omfac	$\frac{\omega_{RMF}}{\omega_c(cyclotronfrequencyato-point)}$
$r_s \equiv$ R	separatrix radius in the z=0 subspace	kappa/κ	$\frac{z_s}{r_s}$
b_0	magnetic field of FRC at z=0 and r = 0	bo	odd RMF magnetic field amplitude
ϕ_0	initial phase of particle velocity in x-y plane	θ_0	initial angle of particle velocity from z-axis
o-point	the magnetic null line on z=0 plane	r_o	radius of o-point
z_{fac}	initial particle z as fraction of zs	r_{fac}	initial particle r as fraction of ro
τ/tau	time in units of cyclotron period at B=b0	escape factor	scale factor from separatrix for escape
energy0/E0	initial energy	escape time	confinement time

Table 23